2019

EXPERIMENTAL AND NUMERICAL SIMULATION OF SPLIT HOPKINSON PRESSURE BAR TEST ON BOROSILICATE GLASS

Mayank K. Bagaria
Michigan Technological University, mkbagari@mtu.edu

EXPERIMENTAL AND NUMERICAL SIMULATION OF SPLIT HOPKINSON PRESSURE BAR TEST ON BOROSILICATE GLASS

By

Mayank K. Bagaria

A THESIS

Submitted in partial fulfillment of the requirements for the degree of

MASTER OF SCIENCE

In Mechanical Engineering

MICHIGAN TECHNOLOGICAL UNIVERSITY

2019

This thesis has been approved in partial fulfillment of the requirements for the Degree of MASTER OF SCIENCE in Mechanical Engineering.

Department of Mechanical Engineering-Engineering Mechanics

Thesis Advisor:	*Dr. Gregory Odegard*
Committee Member:	*Dr. Stephen M. Morse*
Committee Member:	*Dr. Ibrahim Miskioglu*
Department Chair:	*Dr. William Predebon*

Table of Contents

List of figures

List of tables

Abstract

This study is an extension to design of ceramic materials component exposed to bullet impact. Owing to brittle nature of ceramics upon bullet impact, shattered pieces behave as pellets flying with different velocities and directions, damaging surrounding components. Testing to study the behavior of ceramics under ballistic impact can be cumbersome and expensive. Modelling the set-up through Finite Element Analysis (FEA) makes it economical and easy to optimize. However, appropriately incorporating the material in modelling makes laboratory testing essential.

Previous efforts have concentrated on simulating crack pattern developed during 0.22 caliber pellet impact on Borosilicate glass. Major concentration of work is on study of mesh pattern and size. Maximum principal strain has been considered to define the failure criteria which doesn't correspond to theoretical properties. To appropriately incorporate material properties, behavior of ceramics under ballistic impact could be tested through controlled impact Split Hopkinson Pressure bar (SHPB) testing setup.

This paper discusses the results of SHPB bar testing on 1018 cold rolled steel to validate the experimental procedures and result analysis. The work has been extended to conduct testing on borosilicate samples under different input conditions. Strategies for improving the test result are proposed in the paper. The paper extensively covers the dynamics of glass material under ballistic impacts, various test procedures to obtain material model constants.

Incorporating the material model in the previous FEA simulation makes it susceptible to numerous factors affecting the result. FEA characterization of SHPB test makes it suitable for modeling and correlating with the testing result of borosilicate glass. The FEA set-up is simplified to incorporate all the parameters affecting the test. Comprehensive analysis of loading pulse is conducted to validate the model. This paper discusses specimen analysis through standard material model in LS-dyna MAT_110 for five different classes of ceramics. Inconsistences between testing result and simulation have been identified and presented in this paper. The gaps in the study have been highlighted and means to obtain good correlation is proposed in this paper to guide future work.

1 Introduction

Energy consumption in the form of electricity has been a blessing to mankind. It has become such an integral part of our life that little is acknowledged using it. Currently 88% of the human life has access to electricity. All our domestics appliances be it light, fan, electric stoves etc. depend on it. With such an impact it has in everyday life it is very difficult to imagine life now without it. Energy has been powering modern means of transportation and communication and hereby further revolutionizing our life. The key factor affecting its widespread use is the efficiency in transportation. Electricity can be generated at the preferred location and transported efficiently over large distances. Electricity is generated through various energy sources and distributed through various power distribution grid.

The general accepted power form is three-phase alternating current (AC). Distribution grid typically consist of Generation unit, high voltage transmission line, substation transformers and distribution line before consumption. Transformers are typically used for stepping up voltage before transmission line and stepping down before supplied for use. The schematic of the power network is as shown in Figure 1-1.

Figure 1-1: Flow Chart of Electricity Supply Chain

As is evident from the supply chain above, transformer forms one of the essential features of power grid. Transformers typically consist of bushing on the top to guide and protect high powered power lines. Bushing function requires to be mounted on the top of the

transformer. The positioning of bushing makes it vulnerable from long distance, susceptible to open bullet fires. [1] [2] Metcalf snipper attack on April of 2014 in Coyote, California was one such incident where gunmen fired 17 electrical transformers, resulting in temporary blackout with a total loss of $15 million. Along with the loss, the repair took one and half year to retain to its normal functionality.

Bullet impact on bushing can cause fractured glass flying at high speed causing damage to surrounding equipments and injuries to workers. Post event investigation reveals fractured glass façade and windows as major threat in safety of structure and residents. Norway attacks in 2011, shock wave from car shattered all the windows of the Oslo executive government building. 209 out of 325 injuries were result of glass laceration [2].

Bureau of Reclamation manages, develop, and protects water and power supply in southern part of US. They have moved forward to device safety mechanism for incidents like Metcalf Sniper attacks. The functional requirement of bushing to be inert and bad conductor of electricity requires the use of Porcelain as bushing material. Porcelain in itself is inexpensive material but damage caused due to its fragments in bullet impact could be disastrous to the surroundings. Any design modification on the bushing could go a long way in saving the infrastructure from such incidents with insignificant increase in cost.

Mindset for devising the safety mechanism is to fragmentize into small particle under bullet impact. The means suggested that could be adopted for devising this mechanism is by using coating materials or using internal pressure. Though lab testing could be carried out for applying any or a combination of countermeasures. Lab testing is not cost effective because of lot of possible resultant combination. FEA model could be more cost effective option and thereby further would help in optimizing the design. To further cut down on the simulation cost in terms of computing power required, simpler glass geometry with simpler material model has been studied by people working before this work. And then gradually adding complexity to the problem for better prediction of the applied countermeasure.

1.1 Problem Statement

The overall goal of this project is to model brittle glass cylinder that would shatter to pieces upon pellet impact. Crack pattern study and material model definition becomes the key element for the study. Both the factors would provide the prognosis occurring during bullet impact, which can then be closely controlled for achieving the desired result. This project has been carried out with focus on crack pattern study with a simpler material model definition.

A good correlation has been obtained for the crack pattern study, but limited work has been carried out to understand the dynamics of the material at high strain rate of ballistic impact. Thus, this study is primarily targeted to obtain a material model definition which could be applied to the FEA model. The study proposes to use Split Hopkinson Pressure Bar (SHPB) testing for studying the behavior of glasses at high strain rate impact. Modeling SHPB was carried out in LS-Dyna to obtain the material model in reference to available literature. Consequently, the model could be applied to simplified glass model for better correlation with the testing data of actual bullet impact by USBR.

1.2 Current Testing Conditions

As discussed in the previous section, a simpler geometry in the form of test tube is selected for actual bullet impact. Provision is provided to apply internal pressure inside the tube. The set-up is selected to be shot with 0.22 caliper pellet impact. The above condition is chosen keeping in mind elimination of geometrical complexity and its effect on crack pattern. Figure 1-2 shows the lab test conditions on the mounting of the cylinder. In the test set-up, the cylinder is fixed from the bottom and high speed camera are mounted for Side view to capture crack propagation and fragmentation behavior during the impact.

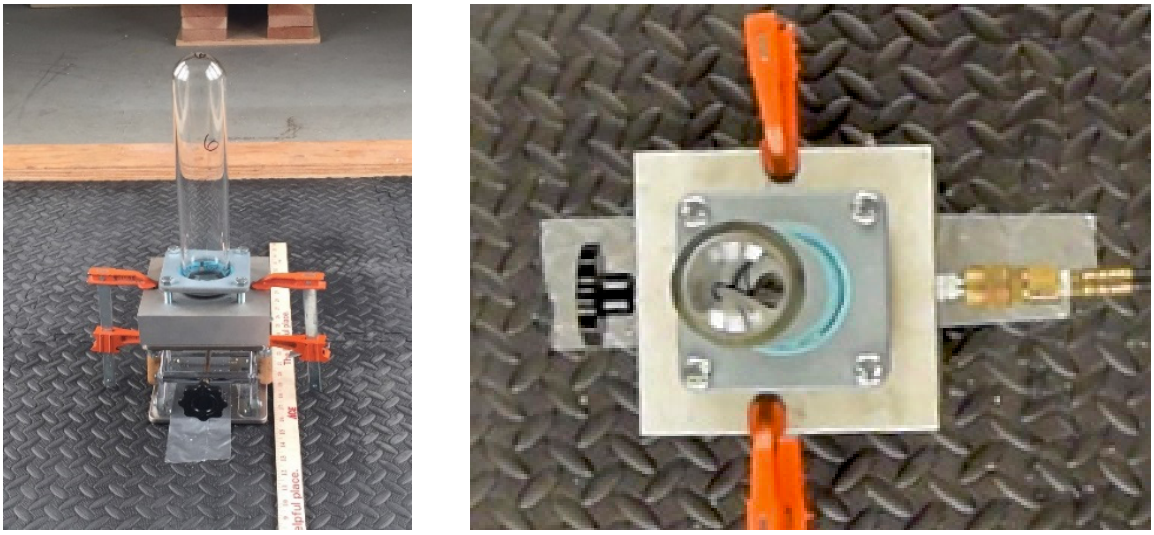

Figure 1-2: Test Condition of Cylinder Mounting [3]

A 0.22 caliber pellet is fired into this cylinder at a velocity of 335.83 m/s (1100 ft/s). The pellet specification include 0.93 g in mass and 5.5 mm in maximum diameter. The shape of pellet is as shown in Figure 1-3.

Figure 1-3: Lab Testing: 0.22 caliber pellet [3]

From the tests, images were captured from the time bullet hits the cylinder tills it leaves from the other side. Figure 1-4 shows the cracking sequence at 0 psi and 100 psi.

[3]Following are the sequence in which the event took place (a) 0 psi sample at impact flash assumed base (0 μs) (b) 0 psi sample one frame after impact flash (67 μs) (c) 0 psi sample after bullet reaches far side (399 μs) (d) 0 psi sample showing ejecta cloud (1596 μs) (e) 100 psi sample at impact flash (0 μs) (f) 100 psi sample one frame after impact flash

(66 μs) (g) 100 psi sample after bullet reaches far side (399 μs) (h) 100 psi sample beginning to separate along length (1064 μs)

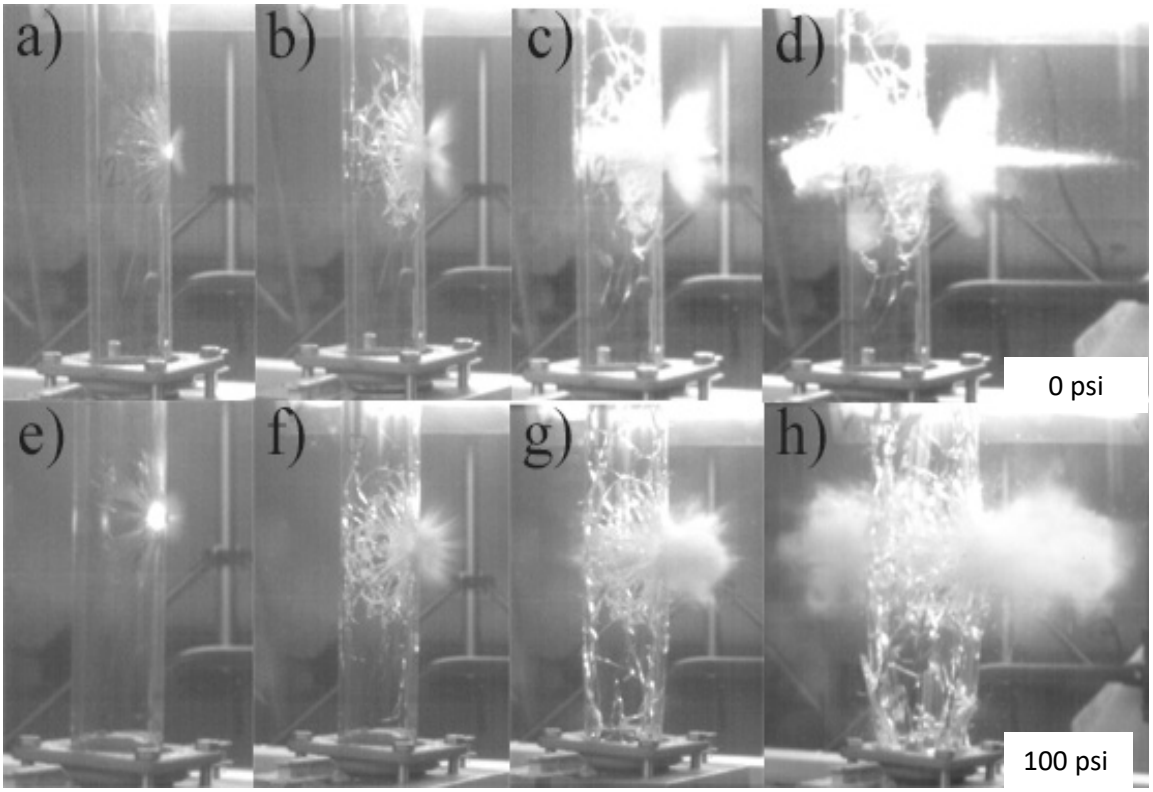

Figure 1-4: Test Condition: Cracking Sequence at 0psi and 100psi [3]

Important observations from images in Figure 1-4: -

Effect of pressure: Pressure seems to have lot of impact in the size of glass particle after impact. As is evident from the images more the internal pressure, more developed will be the cracks and smaller the sizes of the pieces. According to our problem statement, smaller size of falling out pieces is desirable or striving towards pulverization of the sample. Smaller pieces of glass would ensure lesser damage to the surrounding power grid elements.

Form of damage: The area which takes the pellet instantaneously seems to crack on impact. There is substantial propagation of crack in the surrounding element at a very rapid pace. As one moves away from the impact location, the sizes of pieces increases for both testing pressures.

Orientation of cracks: The cracks seem to move in circular direction, near the impact location are radial and takes horizontal and vertical path while reaching the far ends of the cylinder. And the size of the glass shrapnel also increases as one moves away from bullet impact.

1.3 Previous Work

As described in the previous section, three factors needs to be considered for the simulation of test set-up described above. The three factors affecting crack pattern are mesh pattern, mesh size and failure strain. Elaborated study is being carried out by the researchers before this work. Reasonable consideration is also put forward to simplify the model. Previous work with consideration carried out in the project would briefly be described in this section.

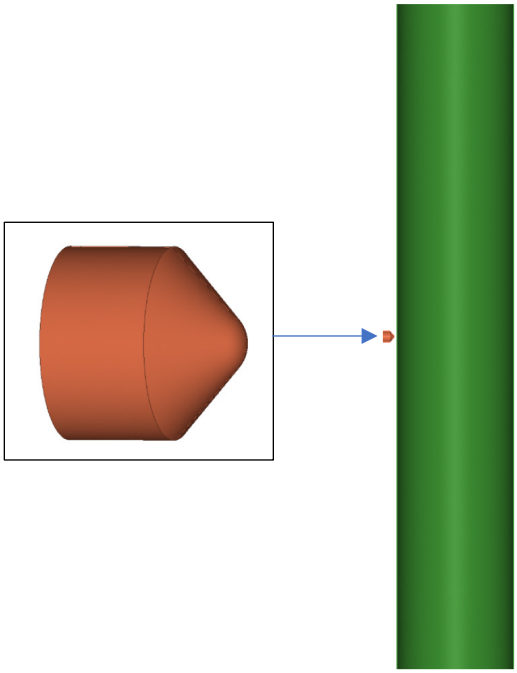

Figure 1-5: Equivalent Simulation Set-up [3]

For modelling the problem statement two components namely pellet and cylindrical tube have to be modelled. The set-up is as shown above, scale is chosen to represent the test set-up. Modelling of each of the component would be described separately and then their interaction would be explained.

1.3.1 Pellet

As shown in Figure 1-6, pellet is assumed to strike in the middle of the cylinder. The physical dimensions area as follows diameter 5.50 mm, mass 0.93 gm, Slope of tip 45 deg and cylindrical part length 3.37 mm. Pellet impact should account to both isotropic and kinematic hardening. LS-Dyna solver material model which is based on both properties MAT_Plastic_Kinematic under MAT_003 is selected. Strain rate effect is not taken into account to simplify the model.

Four node tetrahedral mesh is selected owing to complex geometry and targeted mesh size transition. Based on iterations and to reduce simulation cost, mesh transition is used with increasing size from tip to tail. Smallest element being 0.05 mm on the tip and biggest element of 0.15 mm on the tail.

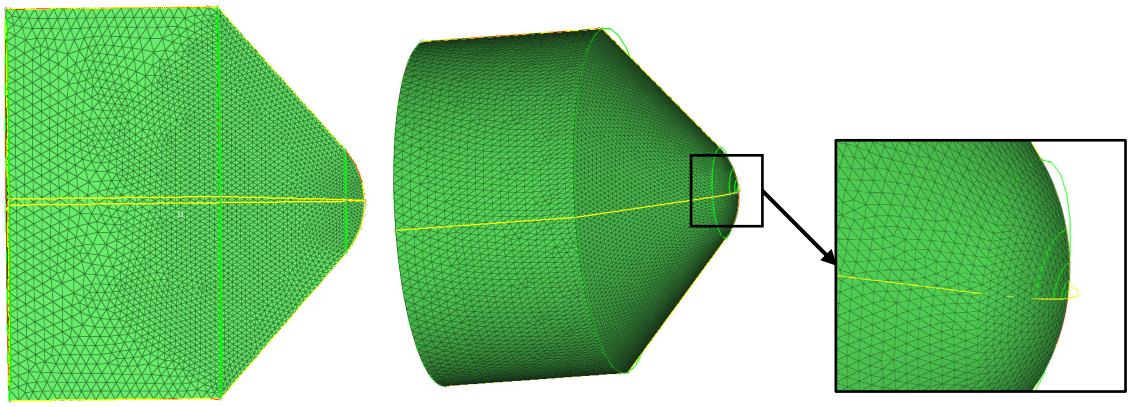

Figure 1-6: Cross- Sectional Mesh View of Pellet [3]

1.3.2 Cylinder

Dimensions of the cylinder is chosen to reciprocate the physical attribute of test set-up. Height is taken as 0.31 m (12 in), thickness 0.635 cm (0.25in), diameter 5.08 cm (2 in) and material pyrex 7740 borosilicate glass. Borosilicate is a brittle material with limited capability to deform plastically. Yield strength is assumed to be 70 MPa, result analysis has shown yield strength to hold less significance. And strain rate based material properties are desirable, but have been limited in previous work. This material model is explicitly being explored in this paper.

The material card chosen is MAT_Laminated_glass which is generally used in industry for safety glasses and windshields. In the test set-up, no such layer is employed. In layer definition thickness is taken as zero making it a useful model for the case. The card offers the following advantage over other cards 1. Failure of material is based on stress strain criteria, 2. Element deletion if plastic strain exceed certain value.

Failure criteria based on 70 MPa gives the strain value of 1.094*10^-3 in/in. The criteria didn't match the condition, literature review [3] suggested to use failure principle strain of 2*10^-6 in/in. Near field study is carried out to calibrate result.

Preliminary mesh analysis suggest that crack pattern is highly sensitive to mesh flow in model. Round grid is chosen at the impact plane, and straight plane for the further point as shown in the photograph. Mesh transition size is taken as 0.5 mm to 1.3 mm. Fine mesh in the impact section and coarse mesh as we move further.

Cylinder is fixed from the bottom edge. Pellet hits the cylinder at 335.28 m/s (100 ft/s.) The cylinder had the provision for pressure loading inside the cylinder.

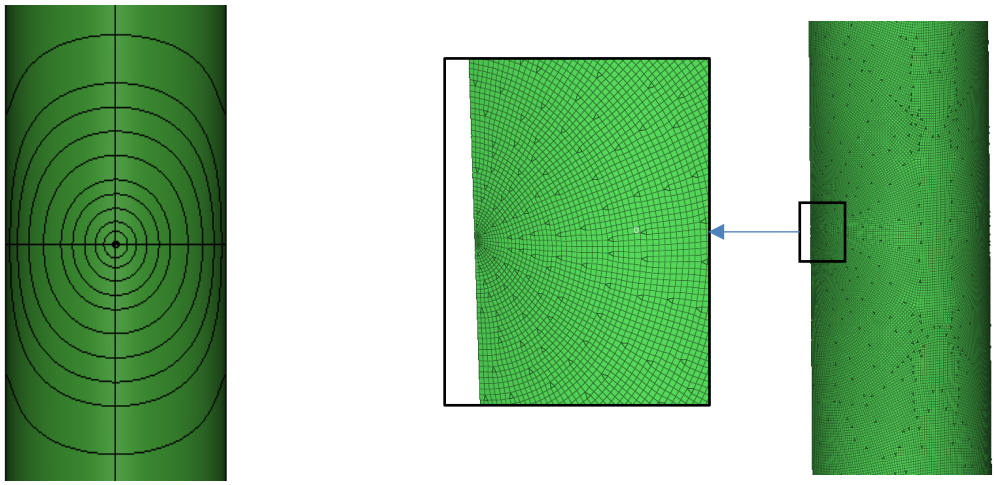

Figure 1-7: Cross-sectional mesh view of Cylinder [3]

1.3.3 Interaction Modeling

Surface to surface interaction gives realistic contact definition. Frictionless contact ensures maximum energy transmission. The interaction is between a 2D and a 3D body and hence SOFT=2 option is used. Due to high velocity impact, high deformation is induced on element. This high deformation may cause distortion and negative volume. Hour Glass mode is included in the model to account for energy change in the model.

Having discussed the brief outline on the model, it is important to understand the failure criteria. Issues in finding failure criteria makes it important to understand the importance of strain rate based model in the underlying problem statement. As discussed above failure criteria is based on principal strain. Lab image correlation is employed to determine the failure criteria. Based on the static properties, material ultimate tensile stress of 70 MPa and Young's modulus of 64 GPa, failure strain comes out to be $1.093e^{-3}$ in/in.

Using model with failure criteria $1.09e^{-3}$ in/in could be simulated with only upto 170 μs. The model shows very stiff response with very few cracks originated by this time. More cracks were found to be developed by this time in lab result snapshots. Principal strain value $3.5e^{-5}$ in/in is determined from static studies at 1psi and $2e^{-6}$ in/in which was used in flat plate impact study during preliminary stage. Near field study was carried out to calibrate the model and correlate with the testing condition. Failure criteria would be reduced by a factor of 10 and crack pattern would be studied.

Choosing failure criteria in the range of 10^{-4} in/in. Model with failure criteria $3e^{-4}$ in/in also shows very few cracks by 500 μs, after pellet leaves second impact surface of the cylinder. Thus the condition is too stiff to generate results similar to lab result. Further reducing the failure criteria to 10^{-5} in/in range. Model with failure criteria $3.5e^{-5}$ in/in shows developed cracks by 500 μs. The cracks are well detailed and well-defined glass pieces are seen separating from the main cylinder body. This is the same criteria used while determining mesh size and mesh pattern in the experiments before this. This matches with the lab result

much better than the other cases. Model with failure criteria $2e^{-6}$ in/in shows very few elements remaining in the simulation at 500 μs. This means other elements have failed already, indicating very fragile behavior.

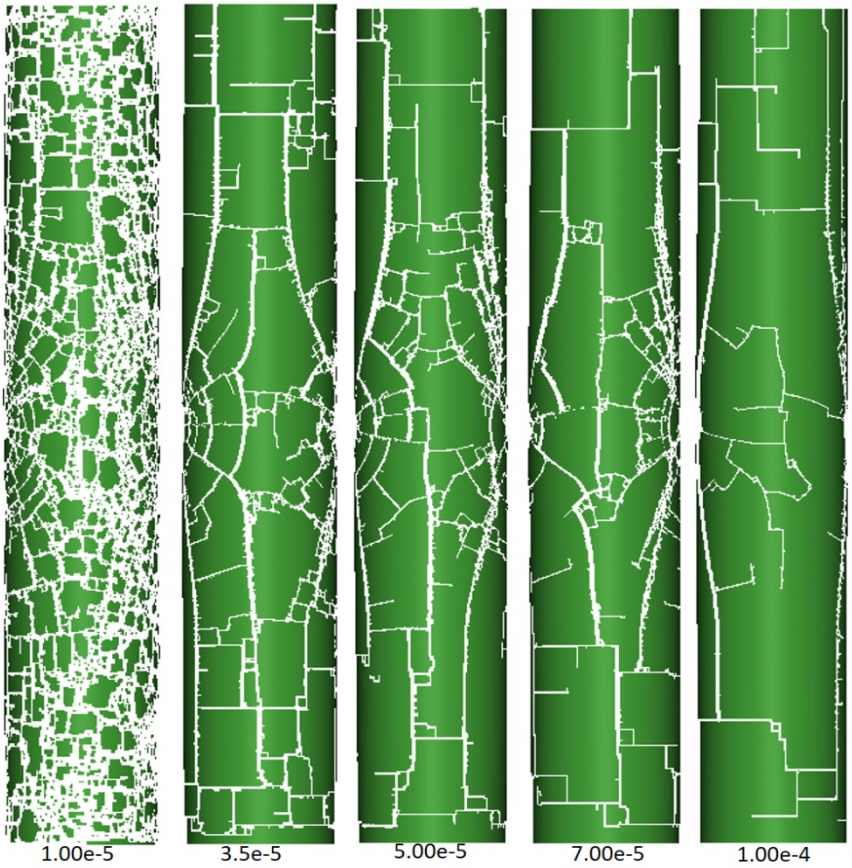

Figure 1-8: Near field Search for Failure Criteria [3]

Thus from these observations, it can be said that failure criterion at or around $3.5e^{-5}$ in/in is best among other range. Near field search around $3.5e^{-5}$ in/in is needed to have more reasonable behavior. The results with value $2.5e^{-5}$ in/in give the most brittle response whereas the results with value $4.5e^{-5}$ in/in give the stiffest response. Results with $3e^{-5}$ in/in, $3.5e^{-5}$ in/in and $4e^{-5}$ in/in are almost identical. However, from a very critical comparison of these 3 results with lab results at 10 psi shown in Figure 6, the results with $3.5e^{-5}$ in/in as max. Principal strain value are most similar to lab results. Thus, even in this iteration the best value of Max. Principal strain value stays at $3.5e^{-5}$ in/in with a tolerance less than $\pm 0.5e^{-6}$ in/in.

Through the failure criteria meets the crack pattern of the testing set-up. It is difficult to explain the selected value of principal strain of $3.5e^{-5}$ in/in. Literature review suggested value off by a factor of 10. As well model is very sensitive to testing conditions. Any change in the input parameter may bring about unpredictable change in the model. So to have a comprehensive model which takes into account all factors and is not sensitive to the input condition, proper material model has to be selected. This paper tend to address the strain based modelling, in an effort to make model less sensitive to failure criteria.

Figure 1-9: Near field search for max. principal strain with $0.5e^{-6}$ interval [3].

2 Dynamics of Ceramics under Ballistic impact

Glasses poses good compressive strength properties however does not develop plastic strain in tension. This differential behavior under varied loading conditions presents a problem in computational correlation. [4] In 2011, Holomquist and Johnson presented a computational constitutive model for numerical analysis of glass subjected to high pressure, large strains and high strain rates. Famously known as Johnson-Holmquist model (JH-2 model), model has been widely used in engineering community for numerical correlation of ballistic impacts.

Before delving deep into the model, understanding dynamics of glass material is imperative. The impact response is quite different for ceramics because of the brittle nature of this material; negligible expansion both in quasi-static and dynamic loading and the influence of hydrostatic pressure on the strength of material. Two distinct dynamic responses observed under different time scale can be observed on ceramic going through a ballistic impact. Phase 1 is the dynamic response is studied in microsecond scale. A compressive wave travelling radially outward is formed right from the point of impact. If the magnitude of compressive wave exceeds the local dynamic strength of the material, damage occurs in the form of cracks. The wave front causes damage in the material radially forming a cone of increasing size. Compressive wave reaching the free surface reflects back as tensile wave causing tensile cracking at spall if the dynamic tensile strength is exceeded. The tensile reflection wave is elaborated in the below paragraph. In Phase 2 the response is studied in much larger time scale of milliseconds corresponding to large scale deformation and capturing of projectile in ceramics. Various material strength properties like dynamic uniaxial yield strength or Hugoniot Elastic Limit (HEL), spall strength and various other parameters comes into play and has to be included in the constitutive model.

Different experimental setups are preferred for testing at varied strain rate. For strain rate above 10^6 /s plate impact test set-up are generally selected. Plate impact spall experiment and laser shock technique have been used by many researchers to characterize internal tensile stresses in glass. Through this experimental tool, characteristics of glass to develop

high internal tensile stresses when not near the surface has been presented. Figure 2-1 shows computed result for plate impact spall configuration demonstration for elaboration on the stated phenomenon. One dimensional analysis uniaxial strain analysis is carried out for the geometry of 1.0 cm glass impactor strikes a 3.0 cm target at V=310 m/s. Mesh resolution of 0.02 cm per element has been selected for computation. The internal tensile strength is assumed to be 1 GPa and with no ability of plastic deformation. Spall plane which is basically the plane which produces maximum tension inside the target, for the given configuration 1.0 form the target rear surface shown in Figure 2-1 (a). Figure 2-1 (b) and Figure 2-1 (c) represents the compressive stress pulse passing though the target at various time. The elastic compressive wave at time t=4.9 μs depicted in black, is propagating from left to right, and has not reached to rear surface of target. At a later time of time t=5.2 μs, wave has reflected off the rear surface and propagating back, releasing the target and begin loading sample in tension. At t=7.33 μs to 7.52 μs, maximum stress of 1.3 GPa is developed at spall plane. Since the target cannot take any plastic strain, failure occur in material. Due to this failure, maximum stress of 1.3 GPa cannot be maintained and attenuates to 70 MPa. Spall plane fails and material around the plane is now governed by 70 MPa. The pulse of 70 MPa propagates through the sample.

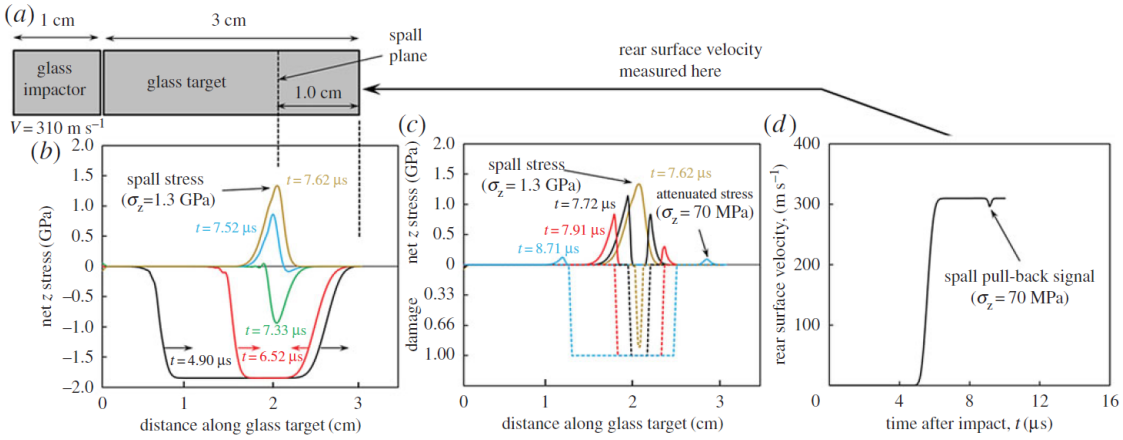

Figure 2-1: Plate impact Spall configuration: (a) Geometry (b, c) z-stress as function of time (d) Pull back signal [4]

In other words, during a pellet impact as in our case, spall strength comes out to be 1.3 GPa. In the spall plane, the strength is very high but strength in the rear surface is as low as 70 MPa. This impact leads to the failure in entire plate by the presence of failure wave.

2.1 Simulation for simplified geometry

The above phenomenon was studied for the simplified geometry to the stated problem. Figure 2-3 shows the simulation state at various time interval under a pellet impact. The simulation is studied under a time interval of 5 µs. For the given computed result, pellet hits the glass at 10 µs. Just upon the impact, the attenuation pulse is formed since the thickness of glass in very less. Element deletion card is used in the simulation, resulting in deletion of failed element. The attenuated pulse moves radially irrespective of the mesh. The attenuated wave propagates at a very high speed and reaches the rear end of the tube before the bullet itself. The crack pattern observed propagates in the radial direction in the center, but due to reflection from another side, crack pattern materializes in the horizontal and vertical cracks along the length of the tube.

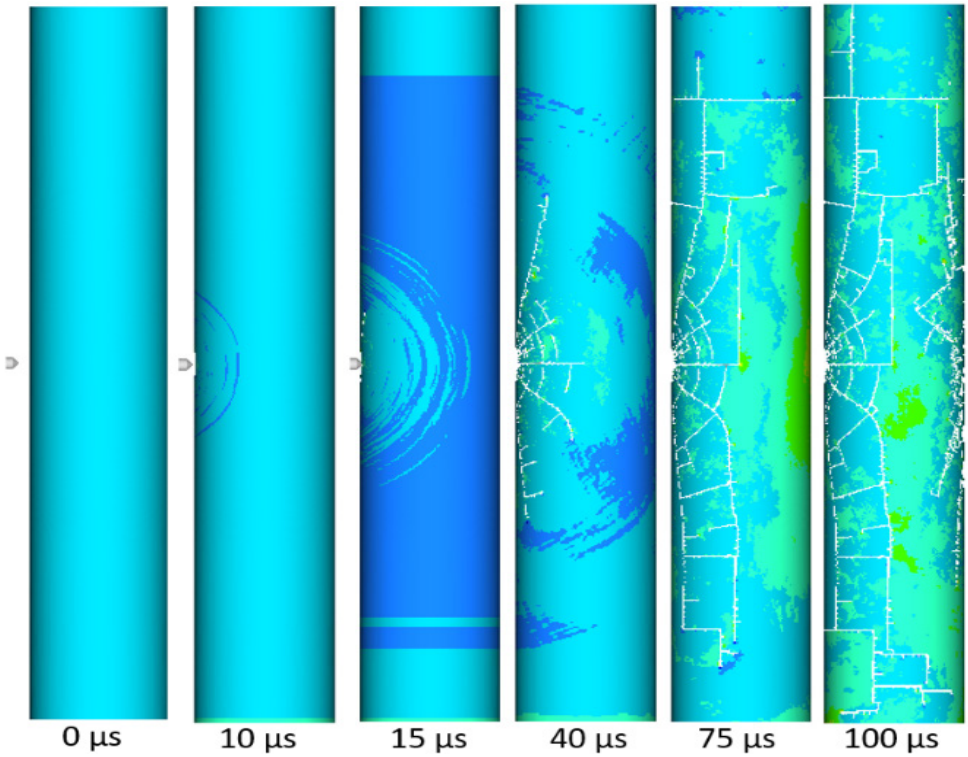

Figure 2-2: Pressure wave behavior: Images from various time section [3]

2.2 Input parameter for material model

2.2.1 Mechanical Properties for Borofloat 33

[5] The characterization for pressure-dependent materials such as sands or concrete is typically conducted through triaxial compression test. Specimen is positioned inside a thick-walled steel pressure vessel, which in turn is placed in an MTS machine. Arrangement is provided in MTS to piston load the specimen through an alumina-loading anvil. Axial force in the plunger is controlled hydraulically. Following the result derived from the test.

Table 2-1: Mechanical Properties of Borofloat Glass [5]

Density	ρ (g/cm3)	2.22
Elastic Modulus	E (GPa)	62.3
Elastic Shear Modulus	G (Gpa)	26
Poisson's Ratio	ν	0.2
Longitudinal Sound Speed	c_L (km/s)	5.61
Shear Wave Speed	c_s (km/s)	3.41

2.2.2 Composition of Glass from X-ray Fluorescence

Table 2-2: Composition of Glass from X-ray fluorescence [6]

Material Composition	BoroFloat-33
SiO_2	80.2
B_2O_3	12.7
Na_2O	3.53
CaO	0.02
Al_2O_3	2.53
SrO	N/A
MgO	N/A
ZrO_2	0.03
K_2O	0.64

2.2.3 Random Network Model

[6] In the random network model, it is often convenient to describe the structure of the network in terms of R, the average number of oxygen ions per network forming ion. For single component glasses such as fused silica (SiO_2) R is the oxygen–silicon ratio and it is easy to see that R is 2.0. For more complex multi-component glasses, R is calculated by dividing the total oxygen by the total network formers on a molar basis. The network can be further described by classifying the oxygen ions per polyhedron as either non-bridging (X) or bridging (Y). Non-bridging ions are bonded to only a single network former while bridging ions bond to two.

Table 2-3: Random Network Model Parameter [6]

Random Network Model Parameter	BoroFloat
R	1.99
X	0.12
Y	3.74

2.2.4 The Griffith Criterion

Pores were identified in Borofloat 33 glass. [7] These pores were found to be located throughout the continuum, generally spherical to mildly elliptical in shape, and ranging in diameter from approximately 0.3–1.0 μm. It is possible to estimate the internal tensile fracture stress using the classical Griffith equation,

$$\sigma_t = \frac{K_{ic}}{Y\sqrt{c}}$$

where, K_{IC} denote fracture toughness where, Y denotes the stress intensity shape factor, 2c denotes the diameter of the internal flaw. For K_{IC} = 1MPa√m, and Y = 1.5 (for a mild ellipse), 2c = 0.3–1.0 μm provides a range in fracture stress from σ_t = 0.94 GPa to 1.72 GPa. The computed internal tensile strength (1.2 GPa) presented earlier agrees with the Griffith criterion in as much as the fracture stresses bound the computed result.

2.2.5 Damage Threshold of Borosilicate glass under plate impact

Flyer-plate impact experiments have been conducted on a borosilicate glass using very-high-speed camera for visual observations, combined with photon Doppler velocimetry (PDV) to measure velocities. [8] The first important result of this work is the fact that we are seeing damage nucleating behind the shock wave at velocities possibly as slow as 130 m/s (compressive stress 0.8 GPa) and for an impact velocity of 170 m/s (l GPa stress). EPIC computations show damage starting at 190 m/s, which was calibrated using a laser spall experiments. These computations provide a spall strength of 1.27 GPa as an upper limit for pulses of 20 ns length. Longer pulses would probably spall the glass at smaller stresses. The stresses generated by the low velocities used in this investigation are well below the HEL of the glass so the HEL cannot be interpreted as a threshold for damage. Clearly the damage grows faster at higher impact velocities; although, when the image is clean, it is not possible to say that the specimen is undamaged. It may be that the size of the damage is microscopic and undetectable with the method being used.

2.3 Johnson Cook Model

Numerical simulation for the modelling of material under high strain rate is gaining ground to make the development cheaper. Owing to the unsafe condition to testing and to improve flexibility. But to rely on numerical simulation, material definition should be accurately defined in software to give a reliable prediction. [9] Ceramic material are of interest for high-energy ballistic impacts due to their low density and high hardness making it suitable for protective armor systems. Under simple loading conditions ceramic may be considered elastic-brittle material. Ceramics behavior under high strain rate is complex with categorizing damage and fracture of paramount importance. While several models exist to describe the behavior of ceramics in high strain loading, Johnson-Holmquist (JH-2) model has been found to provide good correlation, capturing the essential component of ceramic response to ballistic impacts.

Johnson-Holmquist ceramic constitutive model was proposed to address large deformation which was thought to be key parameter for numerical simulation of ceramics. But the

model failed to report progressive damage of the material, and had linear segmentation of model based of pressure and damage conditions. The model was then refined to be less parameter intensive and to cover wide range of loading conditions. The later version of model commonly known as JH-2 overcame the issues faced in previous version, expressing the functions in representation variables.

Microscopic defect dominates the origination of failure in ceramics. JH-2 embodies good correlation with natural phenomenon and computational efficiency through the damage variable. This damage variable records the origin and propagation of failure. The presented work focuses on validation of JH-2 model in LS-Dyna. LS-Dyna code is designed to work in iterative time step function. The deformation in the material profile leads to changes in stress governed by material constitutive equation. And the subsequent state of the material is dependent on the time or path dependent constitutive equation and the variable input from the previous stage.

JH-2 model include four major physical attribute strength model, damage model, strain-rate effect model and state equation. Various equation governing the model in brief would be explained in this section.

2.3.1 Strength Model

Strength required to keep material intact under impact generally referred to as intact strength. Intact strength and strength at fracture both are considered for the strength model. The transition from intact to fractured strength is implemented through damage scalar. The normalized equivalent strength is calculated by

$$\sigma^* = \sigma_i^* - D(\sigma_i^* - \sigma_f^*)$$

[2] Where, D denotes the damage scalar ranging ($0 \leq D \leq 1$), σ_f^* denotes the fracture material strength and σ_i^* is the normalized intact strength. All normalized strength are obtained by dividing the actual equivalent stress by Hugoniot Elastic Limit (σ_{HEL}). The normalized equivalent strength has the common form of:

$$\sigma_i^* = \frac{\sigma}{\sigma_{HEL}}$$

Where, actual equivalent strength has the common form of:

$$\sigma = \sqrt{\frac{1}{2}[(\sigma_x - \sigma_y)^2 + (\sigma_x - \sigma_y)^2 + (\sigma_x - \sigma_y)^2 + 6(\tau_{xy}^2 + \tau_{xz}^2 + \tau_{yz}^2)]}$$

Incorporating strain-rate effect in the normalized intact strength and fracture material strength are defined by the following equations:-

$$\sigma_i^* = A(P^* + T^*)^N (1 + C ln \dot{\varepsilon}^*)$$

and

$$\sigma_f^* = B(P^*)^M (1 + C ln \dot{\varepsilon}^*)$$

Where P^* denotes the normalized pressure given by$\left(P^* = \frac{P}{P_{HEL}}\right)$, P denotes the actual pressure and P_{HEL}denotes pressure at HEL. A, B, C, M, N and T are material constants, T^* denotes the normalized maximum tensile hydrostatic pressure. $\dot{\varepsilon}^*$ denotes the normalized strain rate given by (ε^*=$\frac{\dot{\varepsilon}}{\dot{\varepsilon}_0}$), where $\dot{\varepsilon}_0$ is 1.0 s^{-1} and ln denotes natural log. Equivalent strain rate general form is expressed as

$$\dot{\varepsilon} = \sqrt{\frac{2}{9}[(\dot{\varepsilon}_x - \dot{\varepsilon}_y)^2 + (\dot{\varepsilon}_x - \dot{\varepsilon}_y)^2 + (\dot{\varepsilon}_x - \dot{\varepsilon}_y)^2 + 6(\dot{\gamma}_{xy}^2 + \dot{\gamma}_{xz}^2 + \dot{\gamma}_{yz}^2)]}$$

Test were performed by Holmquist to determine the parameter for the constitutive material model Static split tension, static and dynamic uniaxial compression tests to evaluate intact strength constants. Plate impact test to evaluate Hugoniot Elastic Limit (HEL).

JH-2 ceramic material model was initially developed to simulate high strain impact in the range of ballistic impact and hence its characteristics is not well represented for the tensile zone. But the model is regarded very effective for blast and impact load.

2.3.2 Damage Model

It is very difficult to know the damage level in spite of experimental investigation. Correctly determining the state of damage, strength reduction due to fracture aggravates the problem of finding damage constant. [2] Iterative study is adopted to correctly determine the constant. Simulation with various fracture strength and damage constant were performed to match with the experimental result.

The damage model owing to fracture strength is denoted by:

$$D = \sum \frac{\Delta \varepsilon_p}{\varepsilon_p^f}$$

Where $\Delta \varepsilon_p$ denotes plastic strain, and ε_p^f is the plastic strain to fracture under constant pressure P.

$$\varepsilon_p^f = D_1 (P^* + T^*)^{D_2}$$

Where D_1 & D_2 are the required material constants.

2.3.3 Strain Rate Model

As shown in equation 4 and 5, the stain rate has logarithmic relationship with intact strength and material fracture strength. Figure 2-3 denotes the dynamic tensile and compressive strength with respect to deformation rate. The graph denotes the relation of compressive dynamic increment factor with strain rate. As is clearly visible ceramics strength are highly dependent on strain rate at higher strain rate.

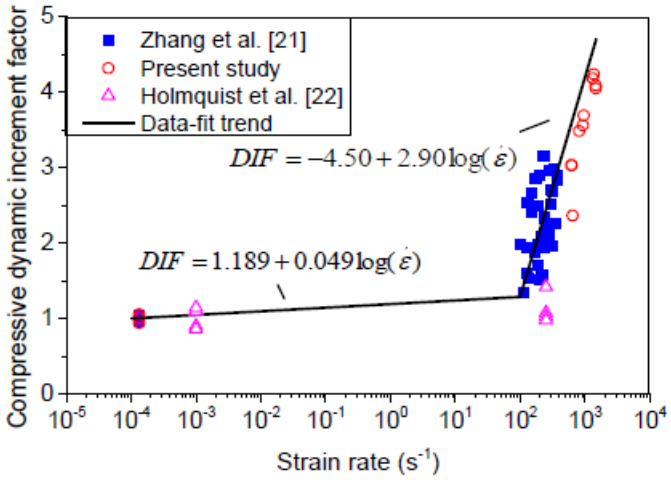

Figure 2-3: Comprehensive Dynamic Increment factor vs Strain rate for Ceramics [1]

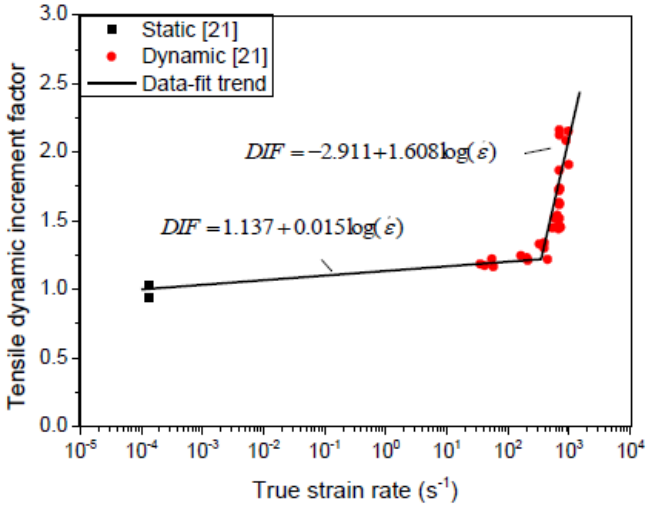

Figure 2-4: Tensile Dynamic increment factor vs True Strain rate for Ceramics [1]

2.3.4 Equation of State (EOS)

Equation of State for glass is defined as

$$P = K_1\mu + K_2\mu^2 + K_3\mu^3 + \Delta P$$

Where K_1, K_2, K_3 are constants, while K_1 is the material bulk modulus. And $\mu = \frac{\rho}{\rho_0} - 1$, which ρ is the current density and ρ_0 is the initial density.

[1] Fracture happens in the form of bulking of material, and this is associated with increment in the hydrostatic pressure. For the calculation this pressure increase of ΔU is associated with potential internal energy. The pressure increase for the time interval (t + Δt) can be associated as:

$$\Delta P_{(t+\Delta t)} = -K_1\,\mu_{(t+\Delta t)} + \sqrt{\left(K_1\mu_{(t+\Delta t)} + \Delta P_t\right)^2 + 2\beta K_1 \Delta U}$$

And the internal energy increase can be mathematically be denoted by:

$$\Delta U = U_{D(t)} - U_{D(t+\Delta t)}$$

In summary, to correctly demonstrate the constitutive equation of a specific ceramic 16 constant have to established to be fed in the software. There are namely 10 constant under the head of Strength constants and strain rate constant are A, B, C, M, N, tensile strength (MPa), Pseudo HEL (MPa), Normalized fracture strength, HEL strength (MPa) and shear modulus (GPa). Damage constants is defined by D1 & D2. Equation of State is denoted by K1, K2, K3 (in GPa) and Bulk.

This study is focused with the implementation and validation within LS-Dyna.

2.4 Material Card Selection for simulation

In general Material Model Plastic strain is one of the main criteria for the simulation problem posed in bullet impact. The main factor describing the behavior of metals undergoing plastic strains are physics of the process, quality and quantity of material. Input to the model may differ according to this parameters.

Dislocation Plasticity model provides the best measure for describing the physics of this plastic strains. This model provides an accurate measure of qualitative and quantitative characteristics. The qualitative feature of this model provide a better visualization that are difficult to obtain practically. For the model described in this paper high speed camera is required to have an image correlation of the effects happening in time scale. Because of

the absence of high speed camera for the experimentation in this paper, qualitative analysis becomes a very nice tool to see the key effect changes. As described above, there are number of commonly used models for plastic strains of metals for example bilinear plasticity model. These models doesn't account to strain intensity i.e. kinematic strengthening phenomenon. The common observation obtained during high strain rate impact is the heat generation during impact pointed out my many researchers in heat analysis of Split Hopkinson Testing. This adiabatic heating of metal in the greatest strained region causes rise in the temperature and hence local softening.

Johnson Cook model as explained in the above section is the most well-known and adopted plastic strain model. This model takes into account both kinematic strengthening and adiabatic heating of the material ongoing strains. However, as described in the above section there are 16 constants value that has to be determined to define the material, difficulties exist in determining the parameter of this model.

The Johnson–Cook model is purely empirical; it makes it possible to take into account the effects of isotropic (static) strengthening, kinematic strengthening, temperature variation and the associated variation in yield strength. According to this model, the stress can most likely be denoted in the single equation through the expression below:

$$\sigma_y = (A + B.\varepsilon_p^n) * (1 + C.\ln\frac{\varepsilon_p'^{\,n}}{\varepsilon_o'})) * (1 - \left(\frac{T - T_r}{T_m - T_r}\right)^m$$

where ε_p is the effective plastic strain, T_m is the melting temperature, T_r is the room temperature, and A , B , C , n , m , ε_0 are the model parameters.

LS Dyna Material Model selection for Glass Specimen

LS-Dyna [10] is primarily chosen for the implementation and validation of study for the model in hand. Many researchers have focused for the numerical validation of Split Hopkinson Pressure Bar test on using LS-Dyna. The software itself provide a good correlation of J-H2 model.

Material model is incorporated in solver through material cards. From the very advent of this software Material card is named as MAT followed by three consecutive number (MAT_001 or is equivalent to MAT_ELASTIC). LS-Dyna manual for material card provides a tabulated version of various material model effects that has been incorporated in developing the material model. There are almost 7 features that has been considered for denoting effects strain-rate effect (SRATE), failure criteria (FAIL), Equation of State (EOS), Thermal effects (THERMAL), Anisotropic/ orthotropic (ANISO), Damage effects (DAM) and Tensile behavior different form compression (TENS).

The tabulated version also classify the material models, in terms of classes of physical materials like for example composite, ceramics, fluid, metal, rubber etc. Based on the various classes and the failure effect requirement of the model, material card for the best fitted material was selected. Total no. of Material Card are 293, Strain Rate Dependent Model are 142, Total Glass Model are 6 and Names of Material Model - MAT 032, MAT 060, MAT 110, MAT 241, MAT 256 and MAT 280.

2.4.1 MAT 032

Using this material model, glass layered with polymeric layers can be modeled. This card is based on the failure criteria. Isotropic hardening for both material is assumed. This material card is based on an assumption that the layer is bonded and assumed to stretch plastically without failure. This model is generally applied to laminated glass and its modeling.

2.4.2 MAT 060

This model was developed to simulate forming of glass products (e.g., car windshields) at high temperatures. This material card is based on strain rate and thermal effect. Forming high temperature account for deformation by viscous flow but provision is provided for large elastic deformations. Viscosity is also defined as a function of temperature making it suitable for treating a wide range of viscous flow problems and is implemented for different

mesh like brick and shell elements. Temperature dependence of Poisson's ratio, Young's modulus, the coefficient of expansion, and the viscosity are represented by Load curves.

2.4.3 MAT 110 & 241

This Johnson-Holmquist Plasticity Damage Model is specifically designed for modeling ceramics, glass and other brittle materials. This complex material card incorporates strain rate effects, failure criteria, damage effects and tension handled differently than compression. MAT 241 corresponds to the original version of the model JH1 and MAT 110 corresponds to the updated JH2 model. The basic difference between models are: - 1. MAT 110 takes into account loading and condition of material, 2. Positon of material whether interior or exterior of the surface determine the strength of that position. 3. Failed material drives the strength in that position making it less mesh intensive. 4. Intact and failed strength also depend on pressure strain rate, thermal damaging softening and effect of third variant.

2.4.4 MAT 256

This material card is valid for isotropic elastic-viscoelastic material model intended to describe the behavior of amorphous solids such as polymeric glasses. This model is based on strain rate effect and differential behavior for tensile and compressive load. This model is based on Bauschinger effect, designed to accurately predict hardening-softening-hardening sequence simulating experimentally observed tensile loading and unloading respectively. The implementation of model is based on hyper-elasticity and uses the multiplicative split of the deformation gradient. This makes the model to accurately predict both large rotations and large strains.

2.4.5 MAT 280

This model is based on Anisotropic/ orthotropic (ANISO), Damage effects (DAM) and Tensile behavior different form compression (TENS). Model allows selection of different brittle, stress-state dependent failure criteria such as Rankine, Mohr-Coulomb, or Drucker-

Prager. The model fail to incorporate strain rate effect that is required for the underlying study.

Studying all the material file and its application in various different scenario, it is evident that **MAT 110** meets our requirement very closely. Problem was cited by Holmquist Paper 2016, that the material model JH1 is heavily mesh dependent and convergence to strong solution. But the new version i.e. JH2 have overcome the issue and have been finding greater adoption for modelling ceramics under ballistic impact. Countermeasure Card MAT 032 could be employed in formulating the counter-measure in form of coated glass.

3 Experimental Section: Dynamic Strain Rates

It is important to understand the nature of the dynamic strain rates experienced in the samples under testing. Lot of natural phenomenon or accidents occurring in our environment call upon strain rate effect. Car collision, concussion sports and ballistic impact are some of the examples. The rate at which strain is being imposed on the target has different magnitude in different scenario. As one may guess, sport based injuries occurs at low strain rate of $10\,s^{-1}$, but is sufficiently large to impact the internal organs. Automotive crash tests induce a strain rate of about $10^3 s^{-1}$on the internal parts. The strain rates achieved in ballistic impacts correspond to the order of $10^6 s^{-1}$.

None of the experimental setup can simulate the strain rate effect for the entire strain rate domain. So, lot of experimental setup or set-up modification is being applied to simulate its effects. The machine or experimental set-up generally used are servo hydraulic machine, specialized machine, Kolsky bar and pressure-shear plate impact.

Considering these strain rates, Figure 3-1 depicts the range of measurement devices that are applicable at various strain rates achieved in the samples.

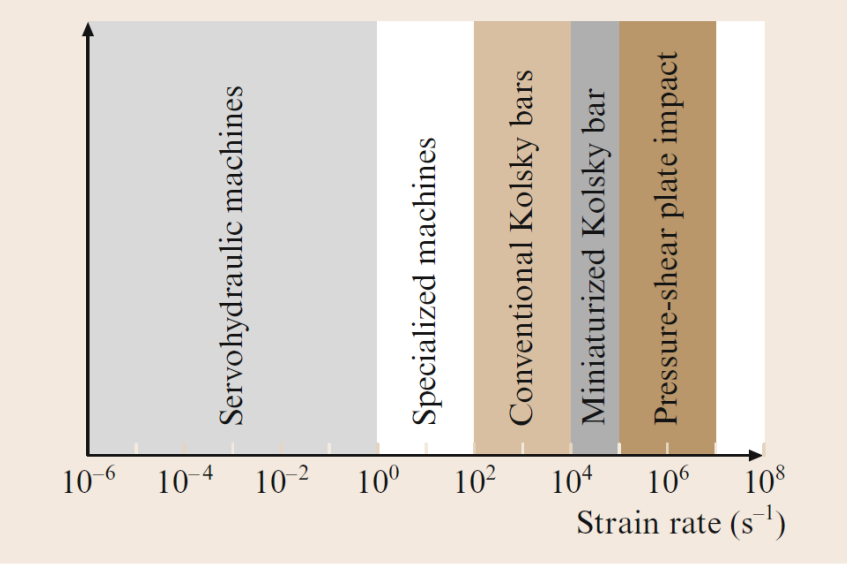

Figure 3-1: Testing Equipment for different Strain Rate [11]

For strain rates higher/lower than the range of operation of the Kolsky bar, approximation methods are required to extrapolate the results achieved from a lower or higher strain rate than required experimental data. Lot of studies indicate that extrapolation result in range of Split Hopkinson gives reasonable approximation for higher strain rate.

3.1 Introduction to Split Hopkinson Pressure Bar Test

The split Hopkinson pressure bar consists of two slender bars with the specimen to be tested placed in between. One end of the pressure bar termed as the incident bar is impacted at a certain velocity with the projectile (striker bar). An elastic wave propagates through this incident bar and reaches the interface between the incident bar and the specimen. Based on the impedance of the bars at the interfaces, part of the elastic wave reflects and part of the elastic wave transmits through the specimen and onto the other end of the specimen. Again, based on the impedance between the specimen and the other bar termed as the transmitted bar, the elastic wave gets partially reflected and transmitted. The subsequent elastic wave propagates through the transmitted bar.

This interaction is depicted in Figure: 3-2.

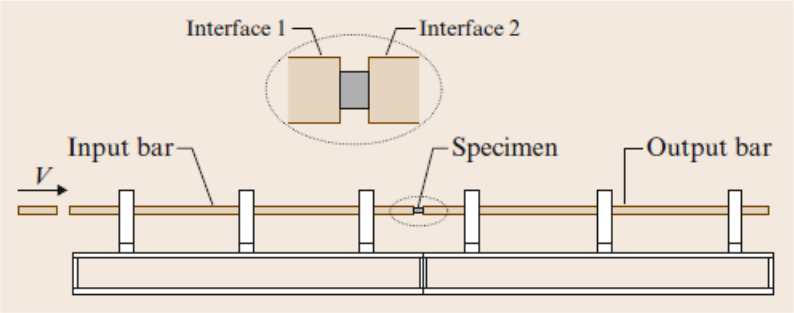

Figure: 3-2: Schematics of Kolsky bar [11]

The elastic wave signals are picked up as voltage readings in the strain gages which are each mounted on the incident and transmitted bar. The elastic wave continues to propagate through the bars while interacting in constructive or destructive interference based on the phase difference between these waves at the point and time of interaction. This longitudinal vibration of roads is related through the following relation to the actual dynamic stress-strain relationship.

$$\sigma_s(t) = E * \frac{A_0}{A} * \varepsilon_T(t)$$

where E is the output pressure bar's elastic modulus, A_0 is the output bars' cross-sectional area, A is the sample's cross sectional area, and is the transmitted strain $\varepsilon_T(t)$ history.

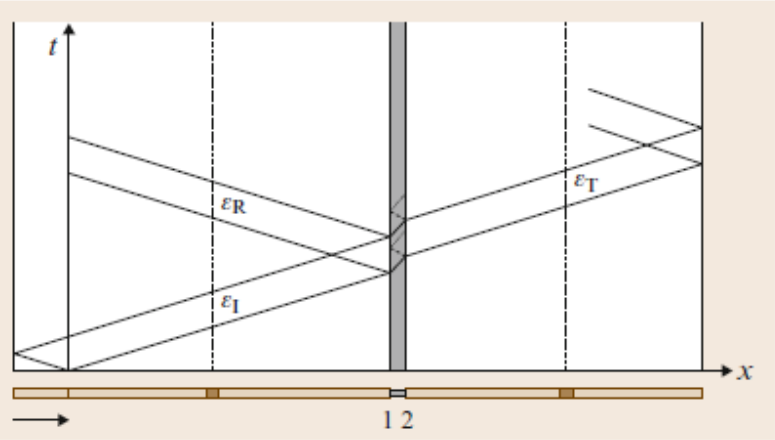

Figure 3-3: Schematic of Stress wave propagation through time and space [11]

The load on the specimen is equal to the average of the two loads at the two interfaces.

Then the nominal stress

$$\sigma_s = \frac{\sigma_1 A_b + \sigma_1 A_b}{2 * As} = \frac{E_b A_b}{2 * As}(\varepsilon_i + \varepsilon_r + \varepsilon_t)$$

Where, A_b denotes the cross sectional area of the bar and $A_s$is the cross sectional area of the specimen.

The nominal strain rate of the specimen is,

$$\dot{e}_s = \frac{\dot{u}_2 - \dot{u}_1}{l_s} = \frac{c}{l_s}(\varepsilon_i + \varepsilon_r + \varepsilon_t)$$

Where, ε_i, ε_t, ε_r denotes the incident strains, transmitted strain and reflected strains respectively.

The following conditions need to be satisfied for validity of the formulation,

1. The elastic waves in the bars must be one-dimensional longitudinal waves

2. The specimen must deform uniformly.

It is worth remembering that the dynamic strength of a material is usually of a higher order to the static strength of the same material. The assumptions related to the Split Hopkinson Pressure bar is that the incident and transmitted bars are elastic in nature and there will be no deformation of the incident or transmitted bar in the dynamic range of operation.

Lubrication is provided to ensure that deformation is concentrated in only one direction.

The wave velocity during its propagation is given as,

$$C_0 = \sqrt{\frac{E}{\rho}}$$

where E denotes the Young's modulus and ρ denotes the density of the material under testing.

The duration of the pulse is dependent on the length of the striker bar and the amplitude of the stress wave is dependent on the velocity of the striker bar.

The above derivations are valid only if the incident and reflected bar are in the elastic zone during testing and the one dimensional wave propagation is valid during the experimentation.

Experimental wave velocity is defined in terms of length of bar and time interval between two wave form. It general form is given as,

Wave velocity= $\frac{2L}{\Delta t}$

Where L is length of incident bar and Δt is the time interval one wave form.

The calibration strain for the gage can be obtained by Calibration Strain = $R_g/(S_g*(R_g+R_c)$
Where S_g is gage factor

R_g is gage resistance R_c is shunt resistance.

The stress and strain in the specimen are calculated from the transmitted and reflected waves, respectively, as follows:

$$\sigma_{specimen} = A_{bar} * E_{bar} * \varepsilon_{transmitted} / A_{specimen}$$

$$\varepsilon_{specimen} = \int \dot{\varepsilon}(t)\, dt$$

$$\dot{\varepsilon}(t) = 2 * c_{bar}\, \varepsilon_{reflected} / l_{specimen}$$

Above equation would be used for calculation form the ΔVo/ V from strain gages vs time to calculate strain vs time.

3.2 Actual Test Set-up: Split Hopkinson Pressure Bar Test

Test setup location: Experimental Stress Analysis Lab, MEEM 702, Michigan Technological University.

Equipment:-

Split Hopkinson Pressure bar Setup consists of two long rods namely incident Bar and transmission Bar with Strain Gage in center. Gas Gun to launch striker bar.

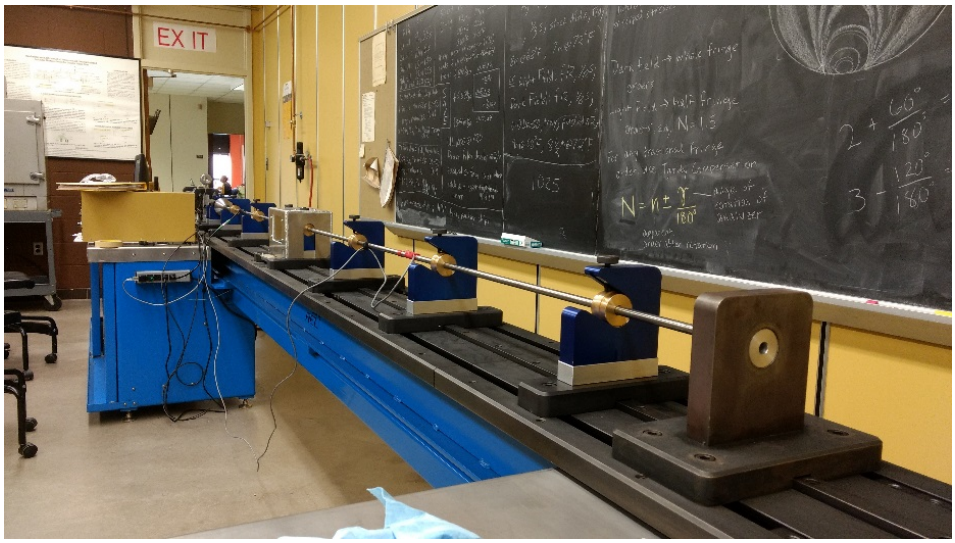

Figure 3-4: Split Hopkinson Pressure Bar Set-up (MTU)

3.3 Technical Specification SHPB set-up

3.3.1 Incident and Transmission Bar

Table 3-1: Technical Specification of bars

Density	0.298 lb/m3
Diameter	0.5 in
Young's Modulus	28*106 psi
Yield Stress	300ksi
Length of Bar	72 in

3.3.2 Strain Gage Data

Table 3-2: Technical Specification of Strain Gage

Resistance	120ohm
Gage Factor	2.14
Length	0.25 in
Voltage Calibration	2V
Shunt Resistance	59.94 kΩ
Gage position on bar	Mid-point

3.3.3 Incidence and Transmission pulse with no bar contact

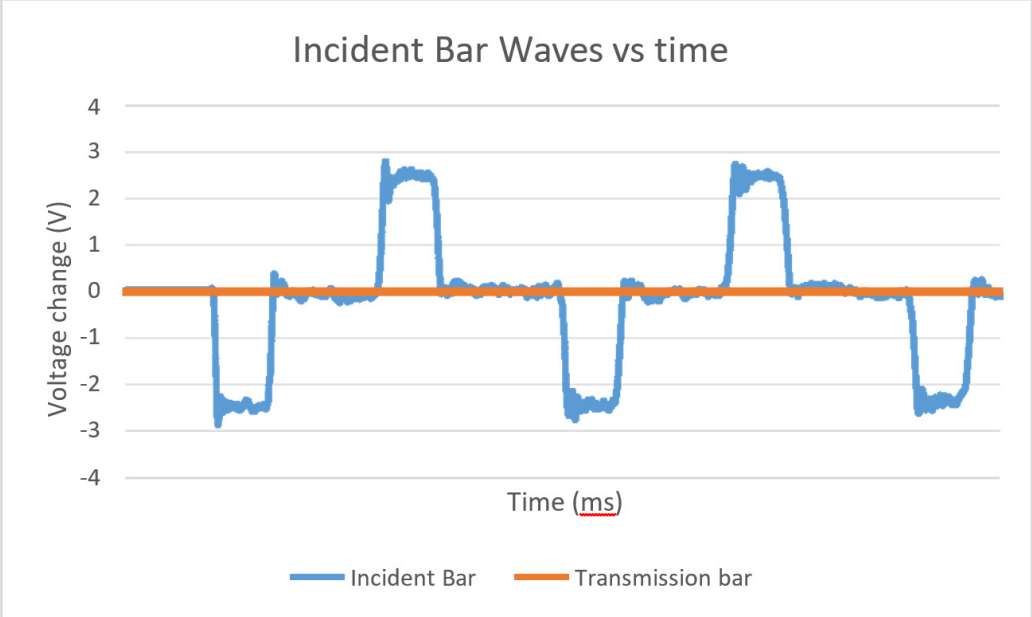

Figure 3-5: Incidence and transmission voltage variation wrt time (Bar not in contact)

3.3.4 Incidence and Transmission pulse with bar in contact

Figure 3-6: Incidence and Transmission voltage variation wrt time (Bar in contact)

3.3.5 Calculation of theoretical and experimental stresses

Experimental Value:-

Amplitude from graph:- Avg of peak value for first square wave form =2.39 V

Calibration Strain = Rg/(Sg*(Rg+Rc) = 942.45 µin/in.

So, Experimental Strain= (2.39/2)*942.45 = 1126.22 µin/in Experimental Stress = E*Ɛ = 217.377 Mpa

Theoretical Value: Amplitude:- 328.283 Mpa

Duration of stress: Theoretical value:-

Δt= 2L/ wave velocity = (2*0.30)/4812.14 = 0.000124s

Experimental value from graph: Δt= 0.000132

3.3.6 Calculation of theoretical and experimental wave velocity

Theoretical wave velocity = $\sqrt{(E/\rho)} = \sqrt{(193.053Gpa/\ 8248.618248.61\ kg/m^3)}$

= 4837.8 m/s

Experimental Wave Velocity= 2L/ Δt = 1.82m/ (0.3797-0.00149ms)

= 4812.14 m/s

3.3.7 Plot of Incidence and Transmission pulse with specimen

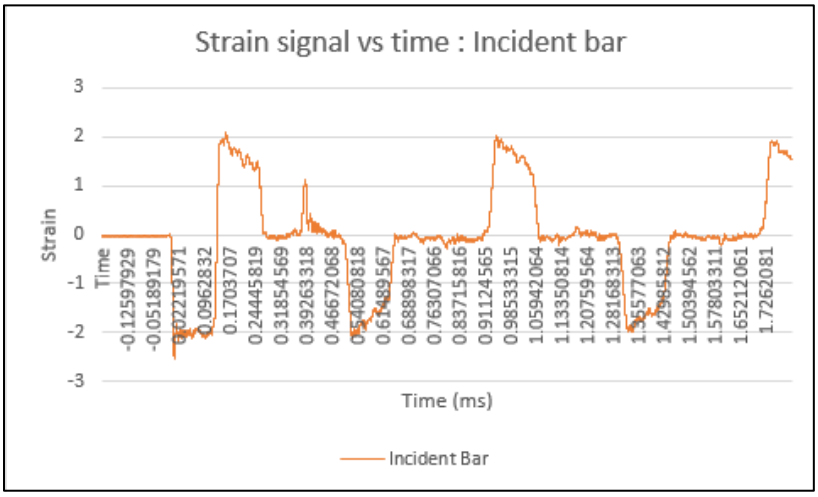

Figure 3-7: Incident Pulse with Specimen

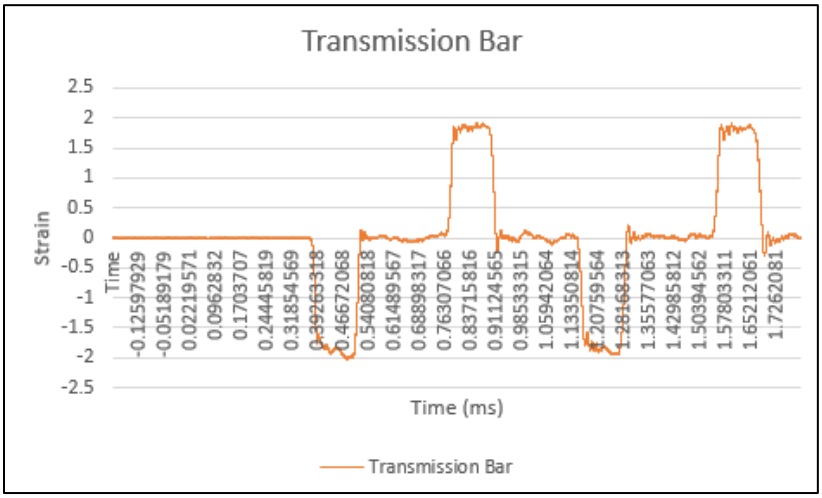

Figure 3-8: Transmission Pulse with Specimen

3.4 Data Processing

The above calculation shows the method for processing the data manually. The analysis for the tested data is done through SURE-PULSE™ [11] developed by REL is used for this paper experimental analysis.

Processing of data in involves following:-

- Creating the bar set-up
- Creating Strain Gage set-up
- Adding strain gage onto the bar
- Incident bar and transmission bar calibration
- Saving/Deleting Bar set-up
- Creating sample
- Loading and trimming data
- Saving and generating graph results.

Typically the graph obtained is used to derive result. For the analysis in this paper, typically following graph is obtained for all testing data strain vs time, stress vs time, strain rate vs time and stress vs strain. The graph obtained from the software seems particularly as shown below. The below curve shows the graph generated by steel sample.

3.5 SHPB result for 1018 Cold-Rolled Steel

Little literature is available for the SHPB testing on borosilicate glass. To have a reasonable and good confidence on the test result, initial testing phase is conducted on a material having rich literature. 1018 Cold-rolled steel is selected for validation of experiment methods, set-up and data analysis. The paper selected cover the strain rate behavior for wide range of strain rate varying from$10^{-3}\ to\ 5 * 10^{4} s^{-1}$. The paper also highlights the innovative method and recommendation for conducting tests.

The experimental parameter for the sample being tested are material: steel round 1018 Cold rolled, testing apparatus: SHPB (MEEM 702, MTU), specimen dimension: length is 0.30

in, diameter is 0.312 in, Striker Bar Length is 9.00 in. and parameter that is variable is pressure: 10, 20, 30, 40, 50, 60, 70 psi. Measurement method is screw Gauge with a least Count of 0.0001 in.

Table 3-3: Observation Table 1: SHPB 1018 Cold-Rolled Steel

Sample No.	Initial Dimension		Input Parameter	Final Dimension		Change in Dimension		Longitudinal Strain
	Length (in)	Diameter (in)	Pressure (psi)	Length (in)	Diameter (in)	Length (in)	Diameter (in)	
1	0.301	0.312	10.000	0.301	0.312	0.000	0.000	0.000
2	0.300	0.312	10.000	0.300	0.312	0.000	0.000	0.000
3	0.300	0.312	20.000	0.299	0.312	-0.001	0.000	-0.003
4	0.300	0.313	20.000	0.299	0.312	-0.001	-0.001	-0.003
5	0.301	0.312	30.000	0.300	0.313	-0.001	0.001	-0.003
6	0.301	0.312	30.000	0.300	0.312	-0.001	0.000	-0.003
7	0.301	0.312	40.000	0.299	0.312	-0.002	0.000	-0.007
8	0.300	0.315	40.000	0.300	0.315	0.000	0.000	0.000
9	0.301	0.312	50.000	0.294	0.317	-0.007	0.005	-0.023
10	0.299	0.312	50.000	0.288	0.318	-0.011	0.007	-0.035
11	0.296	0.312	60.000	0.284	0.319	-0.012	0.007	-0.041
12	0.299	0.312	60.000	0.283	0.322	-0.015	0.010	-0.051
13	0.300	0.312	70.000	0.284	0.322	-0.016	0.010	-0.053

Table 3-4: Observation Table 2: SHPB 1018 Cold-Rolled Steel

Sample No.	Input Parameter	Observation	Data From SurePulse							
	Pressure (psi)	Velocity (ft/s)	Av. Stress	Max. Stress (Mpa)	k	n	Av. Strain	Max. Strain	Av. Strain Rate	Max. Strain Rate
1	10.000	34.230	353.000	381.000	375.980	0.010	0.001	0.002	19.120	138.350
2	10.000	30.450	305.000	337.000	715.460	0.146	0.003	0.004	55.400	309.080
3	20.000	58.470	620.000	785.000	334.110	-0.126	0.008	0.010	129.460	1135.850
4	20.000	55.870	566.000	612.000	594.770	0.009	0.005	0.006	90.408	552.640
5	30.000	69.210	653.000	711.000	679.150	0.008	0.011	0.018	242.130	795.550
6	30.000	65.570	656.000	713.000	870.890	0.057	0.008	0.009	99.120	885.710
7	40.000	78.490	774.000	873.000	723.360	-0.012	0.006	0.009	135.450	431.880
8	40.000	79.740	753.000	797.000	778.830	0.006	0.007	0.011	158.750	445.250
9	50.000	99.150	787.710	957.000	2963.820	0.327	0.021	0.039	381.250	903.690
10	50.000	97.240	818.280	1035.000	2629.370	0.344	0.040	0.060	405.150	1317.120
11	60.000	108.300	814.450	993.000	2053.040	0.241	0.039	0.056	532.320	1302.740
13	70.000	117.800	886.300	1005.000	1222.780	0.095	0.042	0.071	722.200	1627.800

Table 3-3 is based on the actual measurement of sample before and after the testing. The variable parameter is pressure and ranges from 10-70 psi. The velocity is measured from the module mounted in SHPB test apparatus. The strain induced in the sample is 2-5%.

Table 3-4 gives various value obtained in the test. The data method as discussed above is Surepulse, which gives the max. stress, av. Stress, av. Strain, max. Strain, av. strain rate and max. strain rate.

The result obtained is compared to the result from paper. As can be seen from the below graph shows clear strain rate sensitivity at rates exceeding 100 /s. From the above result, strain rate above 100 /s gives average stress in the range (750-886 MPa). The study above provide confidence on the instrument setup, measurement method and analysis of result.

Paper also highlights the strategies for obtaining strain rate for a wide range. The general method for increasing strain rate is through increasing velocity of impact. But a higher rate is obtained by changing the (L/D) ratio. Where L is the length and D is the Diameter of the sample. Typically for our sample analysis ratio is approximately taken as 1. But can also be selected as half and quarter (½ or ¼).

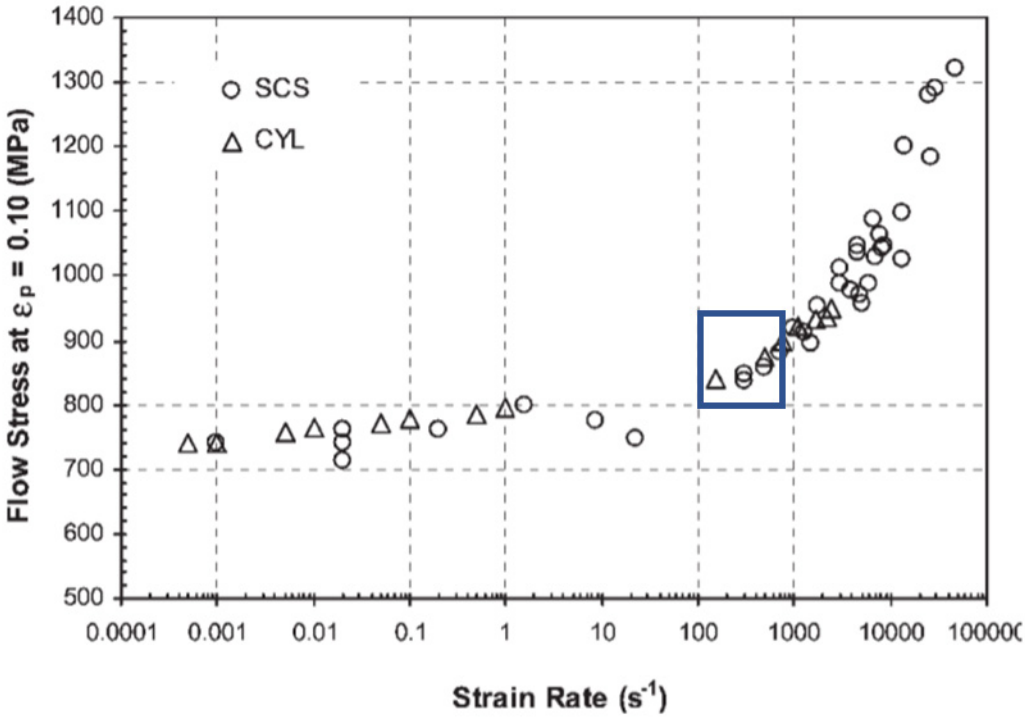

Figure 3-9: 1018 Cold Rolled Steel: Flow Stress vs Strain Rate [12]

3.6 SHPB Test for Borosilicate Glass

3.6.1 Introduction

The problem at hand requires software simulation of pellet impact on borosilicate glass. But since material definition play a huge role in simulation. So, appropriate strain rate dependent model must be ascertained for reasonable result. Problem is aggravated because ceramics strength is highly strain dependent. Stress can vary as high as from 0.8 GPa to 1.27 GPa with impact velocity 130 m/s and 170 m/s respectively. Little literature is available to account for the strain rate dependence for entire range.

Determination of large strain constitutive behavior of materials is a key for modelling of numerous processes such as plastic fracture and high-speed impact. Moreover, the behavior of the material should be determined over a large range of strain rates, as these are well known to influence the overall mechanical response. While a variety of techniques are available for this purpose, the constitutive behavior of a given material is often studied

using various specimens and experimental techniques. Here, one should mention the Kolsky apparatus (split Hopkinson pressure bar) as the main experimental technique for the dynamic characterization of cylindrical specimens in the range of strain rates from 102 to 104 /s.

3.6.2 Test Considerations for Brittle material (Borosilicate Glass)

There is a wide range of materials that can be considered as brittle materials, such as ceramics, glass, ice, rocks, concrete, bricks, cortical bones, and some composites. Under compression, these materials deform in a nearly linear elastic manner and fail at small strain values, typically around 1% or less. Many brittle materials deform in a manner of nearly linear elasticity until failure at small strains.

Brittle materials cannot yield locally, which make them susceptible to stress concentrations. There are three main sources of stress concentrations on brittle specimens are poor flatness and parallelism of the loading surfaces of the specimen, the machining tolerances on brittle specimens are much stricter; misalignment of the bars, which can cause the bar end faces to be unparalleled and thus create stress concentrations at specimen edges even though the specimen has a high machining quality; and specimen indentation into the bar end faces caused by small diameter but stiffer brittle materials, such as tungsten carbide or aluminum nitride, under compression. The stiffer specimen indents into the more compliant bar end faces, generating stress concentrations around the edges of the specimen and causing premature failure.

In order to obtain the failure strength of the brittle material under uniaxial stress conditions, the stress concentrations at the specimen edges must be minimized by dumbbell shaped ceramic specimen and specimen is sandwiched between platens made of hard materials.

3.6.3 Physical Requirement of Glass sample

The specimen diameter should be calculated such that the stress in the transmission bar is less than 30% of the bar yield strength.

Borosilicate Glass compressive strength of approximately 1.00 GPa that is to be tested with 0.5 in. diameter steel bars. The yield strength of the bar is at most 1.20 GPa.

The maximum diameter of the specimen can be estimated to be:-

$d_s = \sqrt{\frac{0.3*1\cdot2}{1}}\ d_B = 0.6 * \frac{1}{2}\ in = 0.3\ in$ (approx.)

A short specimen is desired in order to achieve high strain-rates. For ceramics, a length-to-diameter ratio of 1.0 is more commonly used in Kolsky-bar experiments. Besides the overall dimensions of the specimen, the surface quality of brittle materials, such as glasses and ceramics, is critical to the strength measured in the experiments. The two end faces of a specimen should be flat and parallel.

Due to the sensitivity of the specimen to stress concentrations, the precise linear and angular alignment of the striker, incident, and transmission bars is critically important in experiments on brittle materials. Since brittle materials fail at small strain levels, any misalignment of the Kolsky bar system can result in inaccurate strain measurement.

The specimen should be subjected to a particular stress-wave loading such that it deforms uniformly under a dynamically equilibrated stress state and at a constant strain rate. In most cases, the trapezoidal incident pulse does not facilitate the achievement of these experimental conditions. For example, the brittle specimen may fail at very early stage of loading, e.g., within the first 10 μs. Within such a short duration, the specimen may not be in dynamic equilibrium. Moreover, the specimen may deform at drastically decreased strain rates at the plateau of loading.

3.6.4 Prerequisite for Borosilicate glass SHPB testing

Test specimen dimensions are diameter 0.317 in. and length 0.238 in. Experimental changes to incorporate testing of brittle material are momentum trap for single impact; reducing the frictional impact and ensuring 1-d loading by lubricating the specimen and

Prerequisite for testing is uniform stress in the sample: Using shim between incident bar and specimen.

3.6.5 Impact of shim on borosilicate glass SHPB testing

Pulse shaper is used to achieve dynamic equilibrium condition and obtain constant strain rate condition in test specimen. The effect of shim on dynamic stress on ceramics were studied and result are analyzed. Same size of sample as mentioned above for the glass is used. Result are analyzed for two pressure conditions 10 and 20psi. Based on the pressure, velocity of the impact bar is noted and analysis is being done with SurePulse. Testing are being done with and without shim to analyze its impact. Momentum trap is in contact with the bar to ensure single impact. Due to absence of image correlation, graph generated from SurePulse gives a good measure of the loading at the sample. It also provide the measure of stress growth and stress flow in the sample.

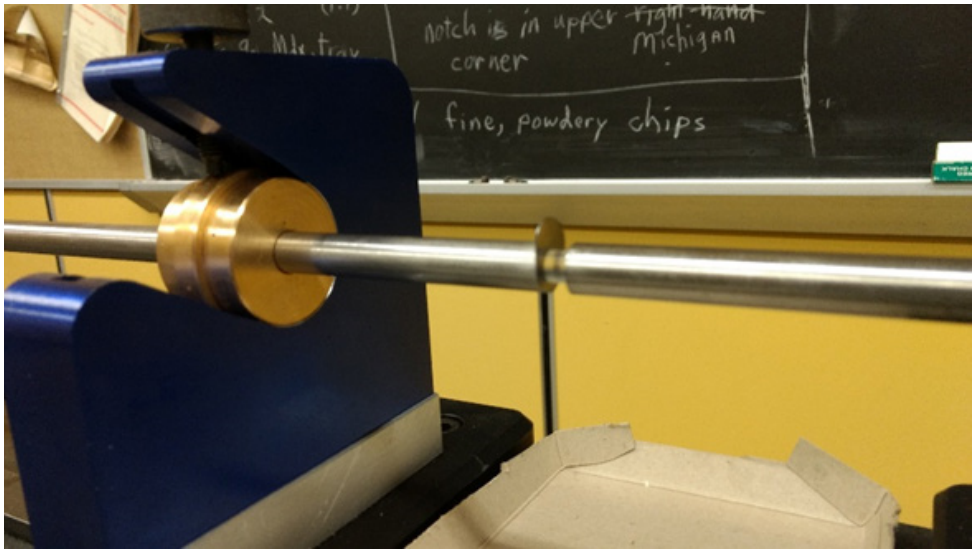

Figure 3-10: Shim and Sample set-up during testing

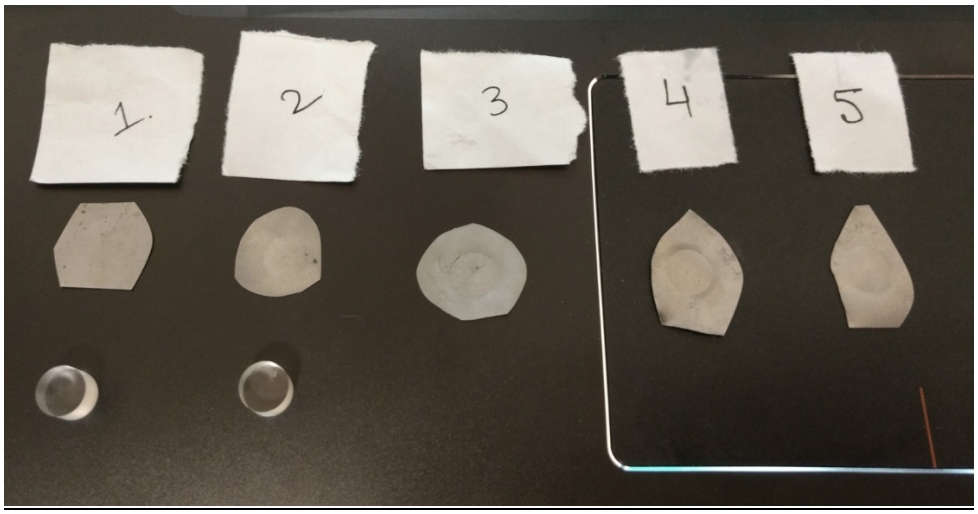

Figure 3-11: Shim and sample condition after impact

Table 3-5: Result of SHPB test result on borosilicate glass with Shim

Sample	Specimen Dimension (in)		Input Pressure		Striker Vel	Strain Rate vs Time	Stress Vs Strain	
	Dia	Length	psi	Mpa	Ft/S	Max (in/in/s)	State	Max. Stress (MPa)
1	0.318	0.238	10	0.069	23.06	900	Crack	96.52
2	0.317	0.237	20	0.138	69.67	1440	Crack	620.52
3	0.317	0.238	20	0.138	56.67	2250	Fail	586.05
4	0.317	0.238	20	0.138	68.31	1925	Fail	620.52
5	0.317	0.238	20	0.138	69.29	1800	Fail	620.52

3.6.6 Study of impact of shim on result

Additional 3 test were carried out with the same parameter without sim.

Sample No.	Specimen Dimension (in)		Input Pressure		Striker Vel	Strain Rate vs Time	Stress Vs Strain	
	Dia	Length	psi	Mpa	Ft/s	Max (in/in/s)	State	Max. Stress (MPa)
6	0.318	0.238	10	0.069	32.05	629	Fail	301
8	0.317	0.238	10	0.069	34.36	1129	Crack	299
10	0.317	0.238	20	0.138	48.67	982	Fail	492

Stress strain curves were compared to understand the behavior and the impact of shim in the testing consideration. Stress strain curve with shim showcased metallic behavior with

stress proportional to strain along with prominent yielding point. Whereas stress strain curve without shim showcased the behavior as expected of brittle material. [12] Literature sources highlights the importance of pulse shaper, but such an analysis is not considered in the study here.

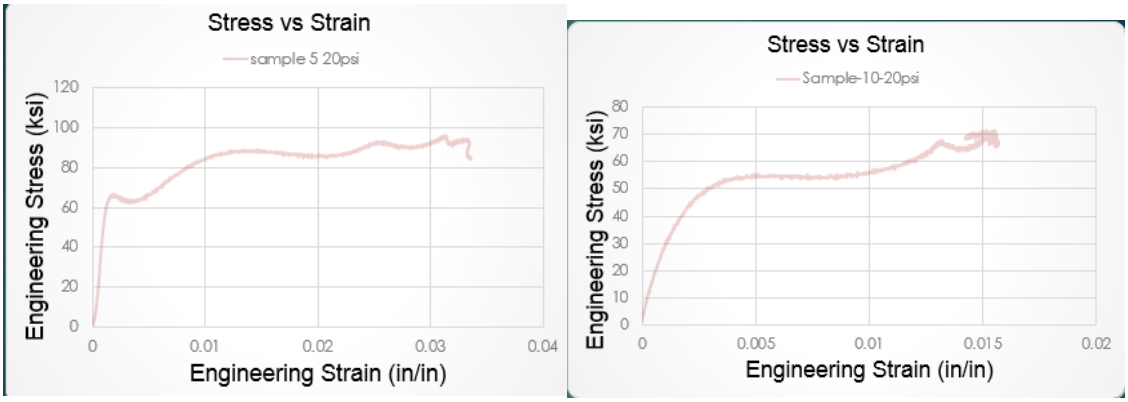

Figure 3-12: Stress Strain curve (a) SHPB testing with shim (sample 5) (b) SHPB testing without shim (sample 10)

For further analysis of the sample shim is not used, because of the interference in the test result. Analyzing the input pulse on the incident which is square wave enough in other word free from distortion and hence use of shim could be circumvented without impacting result.

3.6.7 Testing result for borosilicate glass sample for varied pressure input

The mindset in conducting the test on glass were to obtain the flow stress at various strain rate. The input pressure for the sample is changed to have an increase in sticker velocity consequently affecting the stress pulse magnitude. Dimension of sample is same as for the above shim impact analysis. Striker length is kept constant which impacts the pulse width is also kept constant at 9 in. The pressure input is changed from 10 to 50 psi. The pressure level at which the sample has been tested are 15, 25, 35, 40 & 50 psi. Due to limited sample, 2 samples is used for testing at each pressure. Two of the sample, one at 35psi and other at 50 psi had high increase in strain and failed early during the impact. Those two sample results have been taken away from the paper.

Sample from the shim analysis is also included for having more result files in the graph. A- X series of sample is at 10, 20 from the above study and is without shim. B- X series is the sample tested under this section at varied pressure.

Table 3-6: Observation Table for Glass sample of A & B series

Sr. no.	Sample	Pressure (psi)	Velocity (ft/s)	Max. Stress (Mpa)	Av. Stress (Mpa)	Max. Strain(in/in)	Av. Strain (in/in)	Max. Strain Rate (s^-1)	Av. Strain Rate (s^-1)
1.000	A-1	10.000	32.050	301.000	236.000	0.011	0.007	261.130	173.140
2.000	B-2	15.000	51.190	531.520	449.100	0.010	0.008	847.870	97.662
3.000	B-3	15.000	52.600	552.260	459.400	0.012	0.009	920.640	108.660
4.000	A-3	20.000	48.670	492.000	427.600	0.015	0.013	440.230	118.550
5.000	B-4	25.000	69.170	711.010	618.200	0.011	0.009	1044.520	117.560
6.000	B-5	25.000	69.210	715.450	610.500	0.013	0.010	1191.600	139.610
7.000	B-6	35.000	80.860	951.530	713.700	0.021	0.016	1753.180	211.440
8.000	B-8	40.000	88.610	941.240	765.100	0.023	0.017	1735.040	235.040
9.000	B-9	40.000	87.200	911.200	778.800	0.019	0.015	1538.390	187.390
10.000	B-10	50.000	101.500	1056.300	902.100	0.022	0.018	1870.140	217.020

Visual Observation: All the sample either cracked or got crushed after the impact. Crack were only observed in the sample with lower pressure. Typically for the case in hand, crack were observed in the sample tested at 10psi. Under the tested pressure above 10 psi i.e. 15 psi, all the sample crushed into small pieces above this pressure range.

Following observation can be drawn from the Table 3-6 strain typically in the range of 1-2% is obtained in sample; there is a consistent Av. stress increase with increasing pressure input and strain rate observed in the range of 100-250 /s. Graphs were drawn to observe the trend of the sample result. Av. stress vs strain rate and the same graph were plotted in logarithmic scale.

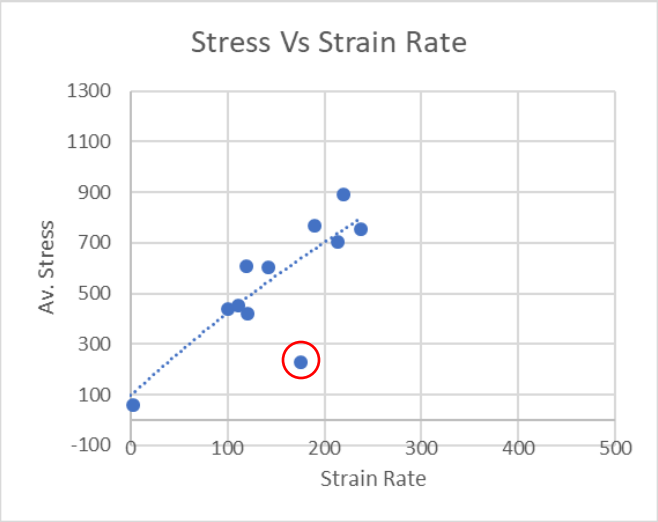

Figure 3-13: Variable Pressure SHPB test result Stress vs Strain rate

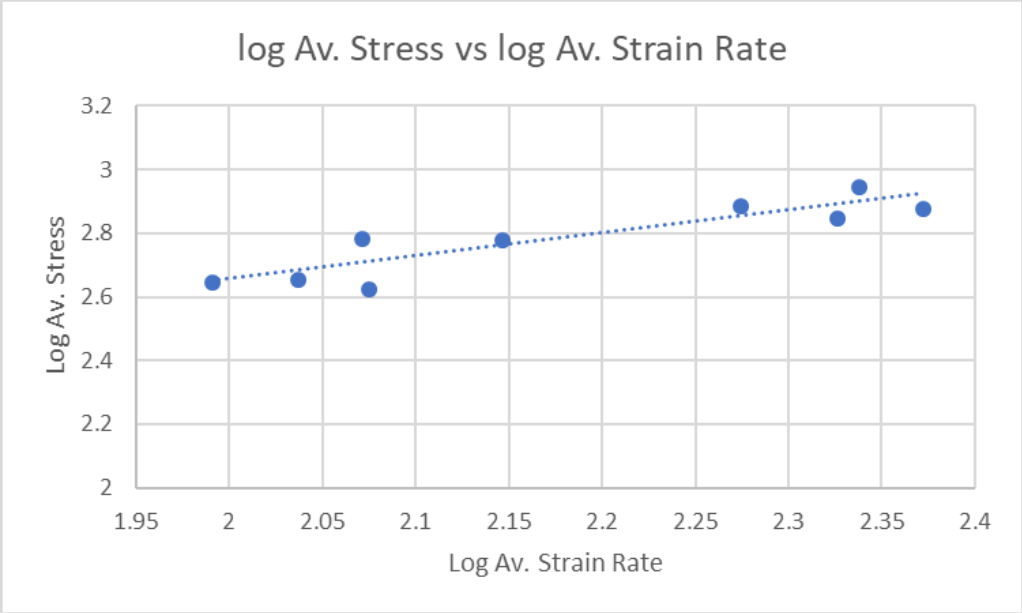

Figure 3-14: Variable Pressure SHPB test result Stress vs Strain rate in Logarithmic scale

3.6.8 Vibrational Study at a particular pressure

General sample size for the testing is taken as 10 samples. Objective was to make the testing cost effective as well as maximize the output with limited sample. Two samples may not be a good representation for the result. To validate the impact of number of sample in the result, several sample were tested at a particular pressure of 25psi. All the testing condition are kept same as the test above only changing the sample size to 5 samples.

Glass sample of B & C series, at a same pressure of 25psi.

Table 3-7: Observation Table for Glass sample at 25psi pressure

Sr. no.	Sample	Pressure (psi)	Velocity (ft/s)	Max. Stress (Mpa)	Av. Stress (Mpa)	Max. Strain(in/in)	Av. Strain (in/in)	Max. Strain Rate (s^-1)	Av. Strain Rate (s^-1)
1	C-1	25	68.720	710.600	628.300	0.013	0.010	1080.340	124.380
2	C-2	25	68.010	691.800	621.620	0.056	0.043	2566.240	735.630
3	C-3	25	67.380	699.000	626.810	0.012	0.010	1034.190	120.750
4	C-4	25	66.860	668.320	603.385	0.020	0.015	1377.610	215.050
5	C-5	25	58.770	652.720	552.670	0.012	0.010	1015.740	133.650
6	B-4	25	69.170	711.010	618.180	0.011	0.009	1044.520	117.560
7	B-5	25	69.210	715.450	610.490	0.013	0.010	1191.600	139.610

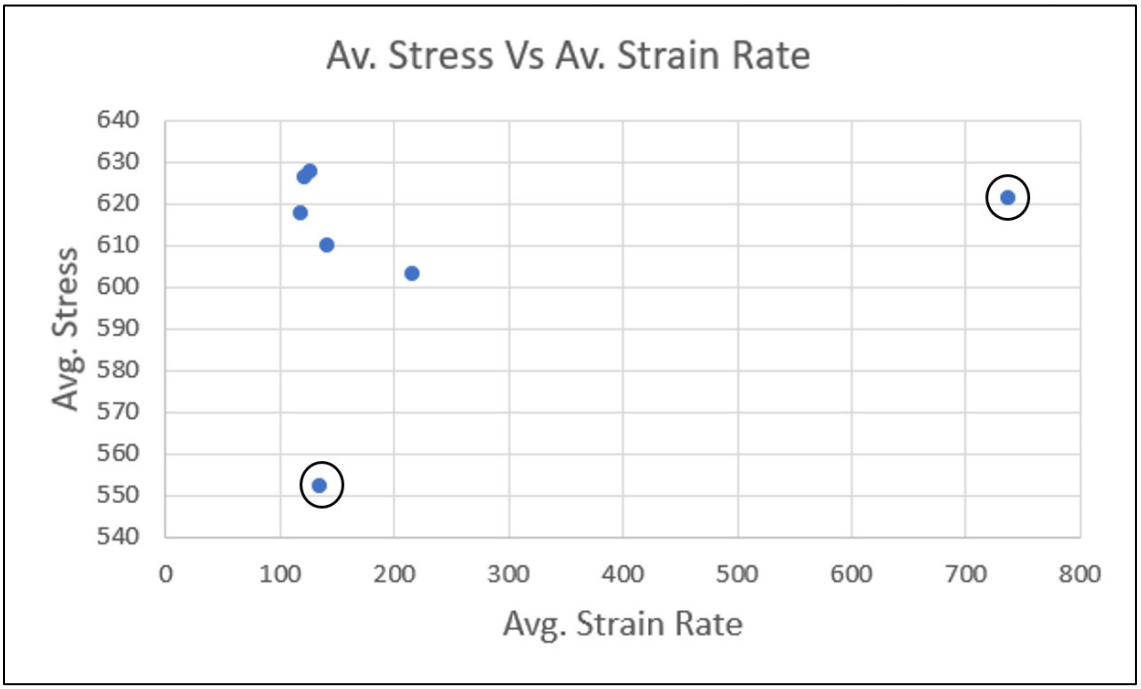

Figure 3-15: Graph of Av. Stress vs Av. Strain Rate

From the curve it is clearly evident, the curve shows two outliers, shown by a dark circle at different stress and strain value. Care has been taken while incorporating all the values in the curve and remove outlier which may have been incorporated due to flaws in lattice structure of borosilicate glass.

Table 3-8: Observation for all Glass sample series (A's, B's, C's)

Sr. no.	Sample	Pressure (psi)	Velocity (ft/s)	Max. Stress (Mpa)	Av. Stress (Mpa)	Max. Strain(in/in)	Av. Strain (in/in)	Max. Strain Rate (s^-1)	Av. Strain Rate (s^-1)
1	B-2	15	51.19	531.52	449.12	0.0104	0.008	847.87	97.6621
2	B-3	15	52.6	552.26	459.44	0.0117	0.0093	920.64	108.66
3	A-3	20	48.67	492	427.6	0.015	0.013	440.23	118.55
4	B-4	25	69.17	711.01	618.18	0.0109	0.0089	1044.52	117.56
5	B-5	25	69.21	715.45	610.49	0.013	0.0104	1191.6	139.61
6	B-6	35	80.86	951.53	713.73	0.0205	0.0156	1753.18	211.44
7	B-8	40	88.61	941.24	765.1	0.0227	0.0171	1735.04	235.04
8	B-9	40	87.2	911.2	778.84	0.0186	0.0149	1538.39	187.39
9	B-10	50	101.5	1056.3	902.12	0.022	0.0175	1870.14	217.02
10	C-1	25	68.72	710.6	628.3	0.0127	0.0104	1080.34	124.38
11	C-3	25	67.38	699	626.81	0.0116	0.0096	1034.19	120.75
12	C-4	25	66.86	668.32	603.385	0.02	0.0152	1377.61	215.05
13	C-5	25	58.77	652.72	552.67	0.0124	0.01	1015.74	133.65

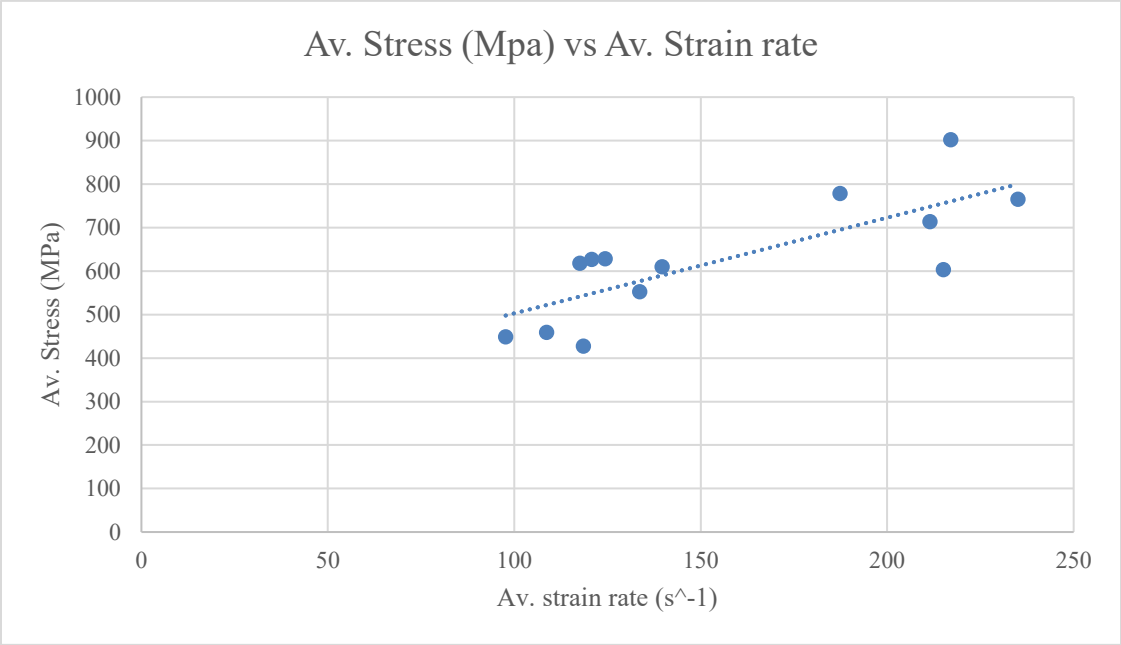

Figure 3-16: Graph with all useful result filtering out outliers

As evident form the curve, trend-line of high slope is obtained. To put into perspective, with a small change in the strain rate range of 100/s (compared to study range of 10^4 /s), Av. stress changes form 500 MPa to 800 MPa.

Prior to starting with the tests, expectation were to obtain the flow stress value for the entire SHPB range (10^2 to 10^4). But the testing yield strain rate at around 1-2.5*10^2. The result obtained range is approximately 2.5% of the entire SHPB range. For future work, strategies mentioned in cold rolled steel to change the L/D could be explored.

Extrapolating result from such a small domain to the ballistic impact strain rate could result in erroneous approximation. To quantify the obtained result, numerical simulation of the set-up is proposed in the paper. The later section highlights the numerical simulation of Split Hopkinson Pressure Bar set-up.

4 Numerical Simulation result LS-Dyna

4.1 Setting up simulation system

Efforts are made to replicate the actual experimental set-up.

Actual set-up basically consist of following component Gas Gun, Striker bar, Incident bar & Transmission bar, Momentum trap assembly, Stopper, Strain Gages, Amplifiers, Bushing for guiding bar and Specimen.

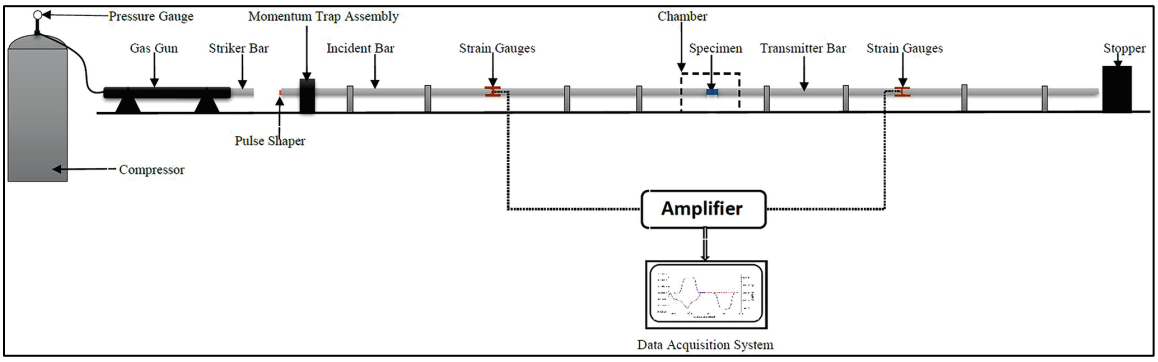

Figure 4-1: Schematic of Split Hopkinson Pressure Bar test [13]

Adaptation for Simulations are as follows (a) Gas Gun: Velocity is imparted to all the nodes of striker bar (b) Striker Bar: Geometry is created as per the dimension of the bar used in the testing (Indicated in blue color Figure 4-2: Simulation set-upFigure 4-2), (c) Incident and Transmission Bar: Geometry is created as per the dimension of the bar used in the testing. (Indicated in pink and brown color respectively in Figure 4-2). (d) Momentum Trap: Set-up is not fixed, causing it to impact just once the sample, (e) Stopper: Simulation is run for 5ms, but can be further reduced to 1.2ms to record all the required pulses, (f) Strain Gages: - Strain gage is mounted in the mid-section for our set-up. Plane containing strain gage position is marked for reference in the model. Strain gage analysis is discussed broadly in the later chapter. (Indicated by the teal color plane on the bar in Figure 4-2), (g) Amplifiers: Test data is received from the software itself thereby amplification is not required. But converting in the required format is carried out. This has also been discussed broadly in later sections, (h) Bushing: It is required to keep the bar in one direction. It is ensured by constraining the body to move in only one direction. In our case z axis is allowed axis of motion, all other axis is constraint to move and (g) Specimen: It is assumed

that the sample is mounted in the center of the bar. Same has been ensured during the testing. (Figure 4-3 shows the sample, mounted in between the sample).

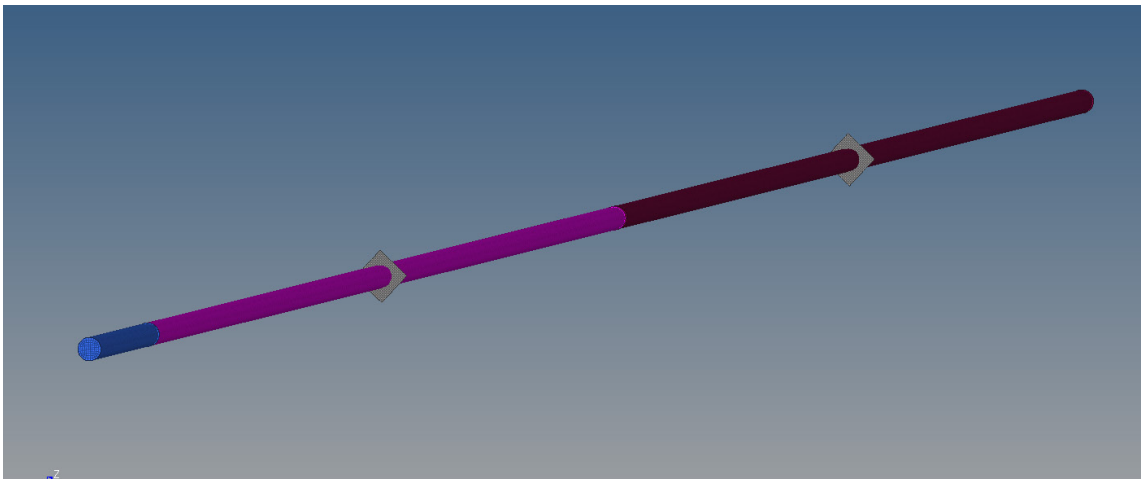

Figure 4-2: Simulation set-up

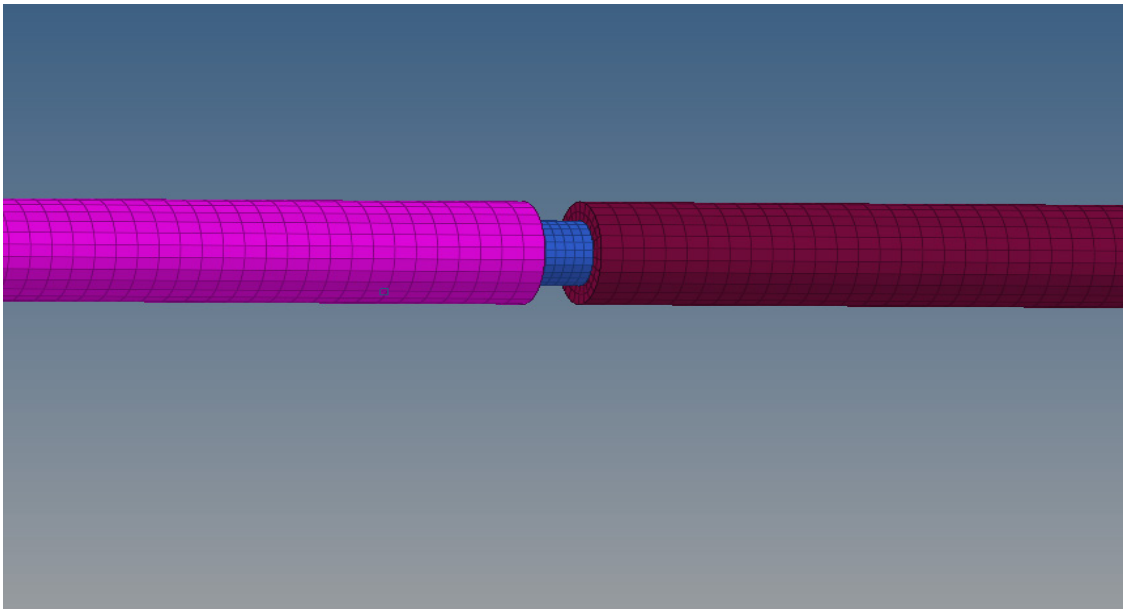

Figure 4-3: Specimen and Bar positioning

4.2 Dimension of various bar

Table 4-1: Dimension of Incident and Transmission Bar

Shape of bar	Cylindrical
Length	72 in
Diameter	0.5 in
Thickness	Solid

Table 4-2: Dimension of striker Bar

Shape of bar	Cylindrical
Length	9 in
Diameter	0.5 in
Thickness	Solid

Table 4-3: Dimension of Specimen

Shape of specimen	Cylindrical
Length	0.238 in
Diameter	0.317 in
Thickness	Solid

4.3 Load Collector

Load is applied two basically in two forms namely velocity to striker bar: All the nodes is moved towards the incident bar with the input velocity. The pressure change corresponds to velocity of striker bar in the SHPB. Velocity corresponding to pressure is recorded in the SHPB set-up. This velocity is directly fed in the simulation and is the change input condition for the simulations; gravity to the model is defined as constant magnitude of $9.8\ m/s^2$. This is defined to account for the sample falling after the specimen is set free. But based on the simulation result, gravity parameter can easily be dropped since the test time is negligible to be dominated by gravity.

4.4 Contact Definition

The contact definition is defined as Contact_automatic_suface_to_surface contact. The definition is provided in pair depending on the position in the set-up. First pair of contact is between striker and incident bar, second pair is between incident and specimen, third pair is between specimen and transmission bar.

Material definition:-

For the bars material model is taken as MAT_003_PLASTIC_KINEMATIC card. This model well include isotropic and kinematic hardening plasticity. This card is based on strain-rate effects and failure criteria.

Table 4-4: Material Property of Incident, Transmission and striker bar

Bar Selected	Incident, Transmission, Striker bar
Density	0.298 lb/in^3
Young modulus	28* 10^6 psi
Yield Strength	300 ksi
Poisson's ratio	0.3

Specimen: - Material to be selected for specimen is MAT_110 also known as MAT_Johnson_Holmquist_Ceramics. The model has been explained broadly in the material model section of this paper. There are 19 constant which has to be selected for this model. The value to be taken for material model is explained in the later of this paper. Basically five class of ceramic is being taken and material model is obtained from the literature.

Control Energy Card: Hourglass modes are nonphysical, zero-energy modes of deformations that produces zero strain and no stress. Hourglass modes occurs only in under-integrated solid, shell, and thick shell elements. LS-Dyna has various algorithm for inhibiting hourglass modes [3]. Hourglass energy & energy dissipation is computed and included in the simulation.

4.5 Strain Gage Analysis

Strain Gage used in the experiment has following specification

Table 4-5: Strain Gage Specifications

Resistance	120 Ω
Gage Factor	2.14
Length	0.25 in
Voltage Calibrated	2V
Shunt Resistance	59.94 kΩ
Gage Location	Midpoint on each bar

In the experimental set-up the strain occurring in the bar is recorded through strain gage. The voltage reading of this strain gage is amplified through Wheatstone bridge. The time frame of data recording is very fast in the order of $1.25*10^{-5}$ ms.The incident pulse, transmission pulse and reflected pulse combined together gives the required result. As mentioned in the experimental section of the paper.

To correlate with the testing conditions, similar assumption is taken for the simulation. 3 element as shown in Figure 4-4 corresponds to 6.853mm (0.269 in). This 3 element is chosen in the bar near the strain gage section. Stress and strain is proposed to be studied in this element to obtain stress and strain vs time curve.

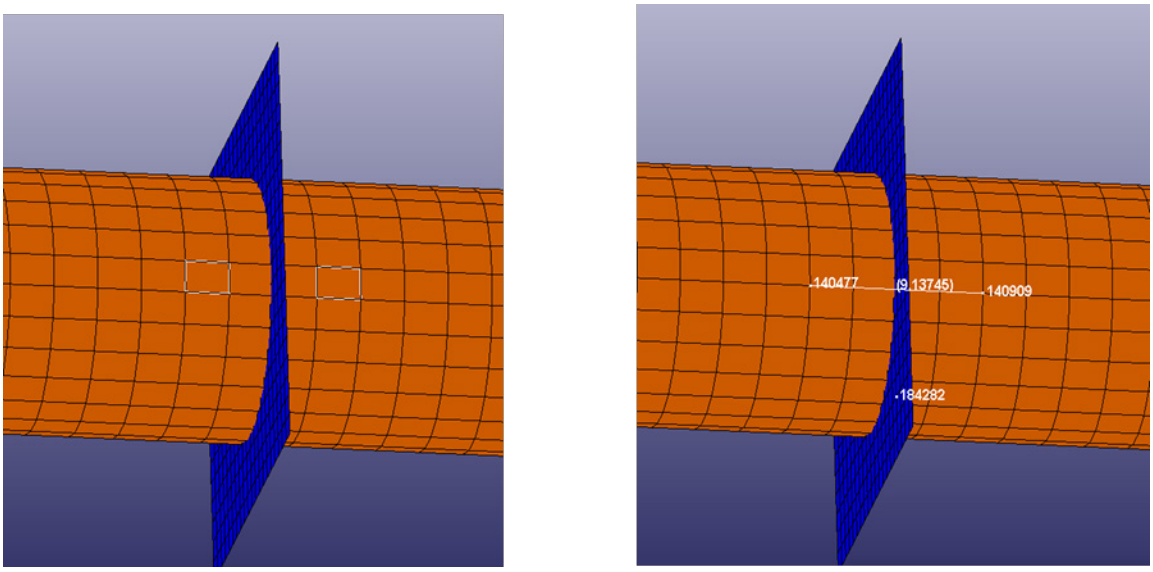

Figure 4-4: Element Selection for strain Gage Analysis

4.6 Stresses in Bars

Initial study suggest that the stress change because of the adjacent element is not very significant and hence instead of three element only two extreme elements are taken. Stress is studied for both incident and transmission bar. Only the magnitude is being considered, so the graph doesn't differentiate between compressive and tensile stress. Figure 4-5 shows the value obtained and behavior of different pulse. Since the stress in the two element of a bar is very close, so there is an overlap between the pulses.

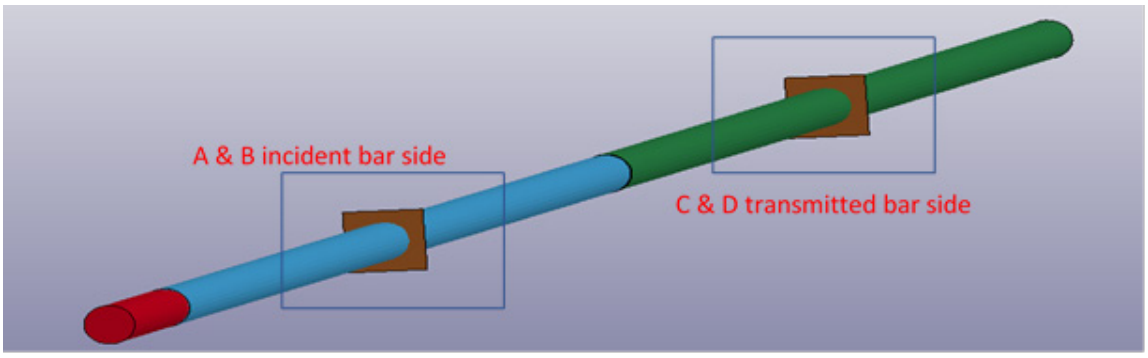

Figure 4-5: Element definition for stress analysis

4.7 Strains in Bars

Similar analysis is carried out for strain as has been carried out for stress. But since the strain cannot easily be obtained from the LS-Dyna software. So, displacement of the node in z-axis is obtained with respect to time. Based on this displacement, differential strain can be obtained between the nodes. The governing formula is for Strain would be $\frac{\Delta v}{AB}$, where Δv is the difference between distance between node A & B, and AB is the length between A & B node which in our case is 6.853mm (0.269 in). Plotting the strain vs time graph gives curve as shown in Figure 4-6.

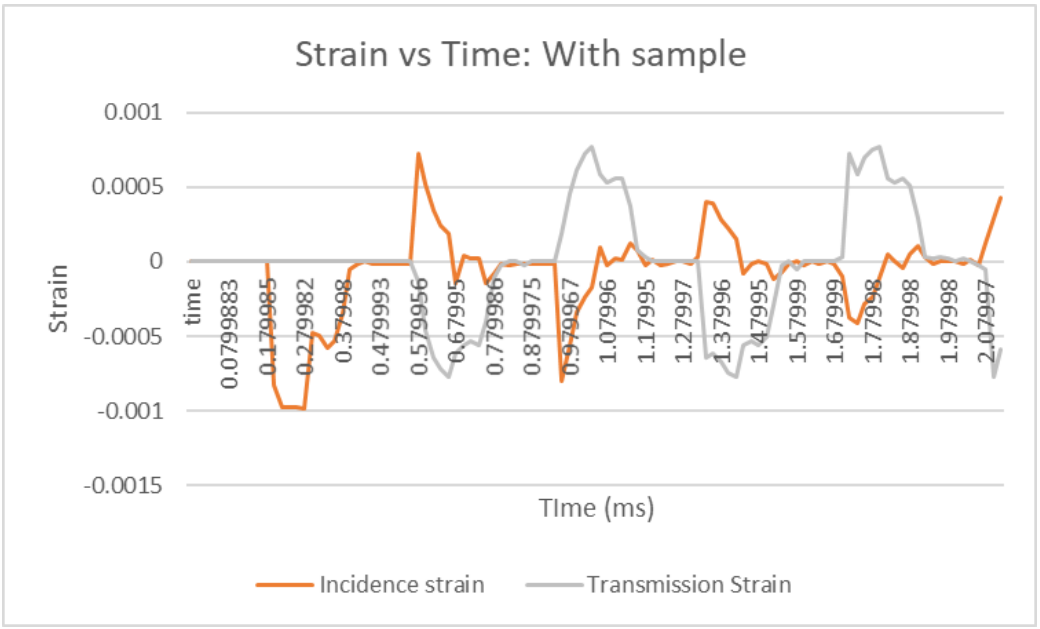

Figure 4-6: Strain vs time graph with Specimen

4.8 Comparison of Experimental and Simulation result

Conducting initial simulations and incorporating changes in the model, incident pulse was analyzed. Before starting with the analysis of the sample, it is very important to analyze the incident pulse. The incident pulse decides the loading on the sample. Key was to match the superimposition to look at the difference in the magnitude and pattern of the pulse. Striker velocity recorded during the testing is fed in simulation. To simplify the model, sample is removed. Test as well as simulation is conducted with incident and transmission bar together in contact.

As described above the data in testing is recorded in timeframe of $1.25*10^{-5}$ ms. In simulation the time step is $2*\ 10^{-2}$ ms. Pulse time frame with 9 in striker bar is 0.16-0.2 ms. So, for the same time frame 16000 data point is recorded in test and only 10 point in simulation. Efforts are made to have more data point for simulation in the succeeding sections. But during comparison less data point is recorded in simulation, which may lead to abrupt change in profile of curve.

Efforts are made to derive a multiplication factor for ease of analyzing different results. Data used in the calculation is taken from Table 4-5. Basic calculation for converting the test data in the form of voltage vs time curve to Stress vs time curve is shown below.

Calculation for experimental results:-

Calibration strain = $\frac{R_g}{(S_g*(R_g+R_c)}$ = 942.45 μ in/in.

This calibration strain corresponds to 2V reading strain.

So for a reading of 2.39 V, strain = $(\frac{2.39}{2})$ * 942.45 = 1126.22 μ in/in.

Experimental Stress = E* Ɛ = 217.377 MPa

So, multiplication factor = Mf = $(\frac{Calibration\ Strain}{2} * young's\ modulus) = 90.971$ MPa/V.

Stress at all instance can be found by multiplying Mf with voltage reading. Since the multiplication factor is a constant, hence there is no change in the trend of the curve.

Calculation for the simulation data:-

Strain is calculated as described in section 4.7. The graph obtained is strain vs time graph. It fairly simple to convert this curve to stress vs time graph. Young modulus is the multiplication factor in this case.

Superimposition of two curve gives following result.

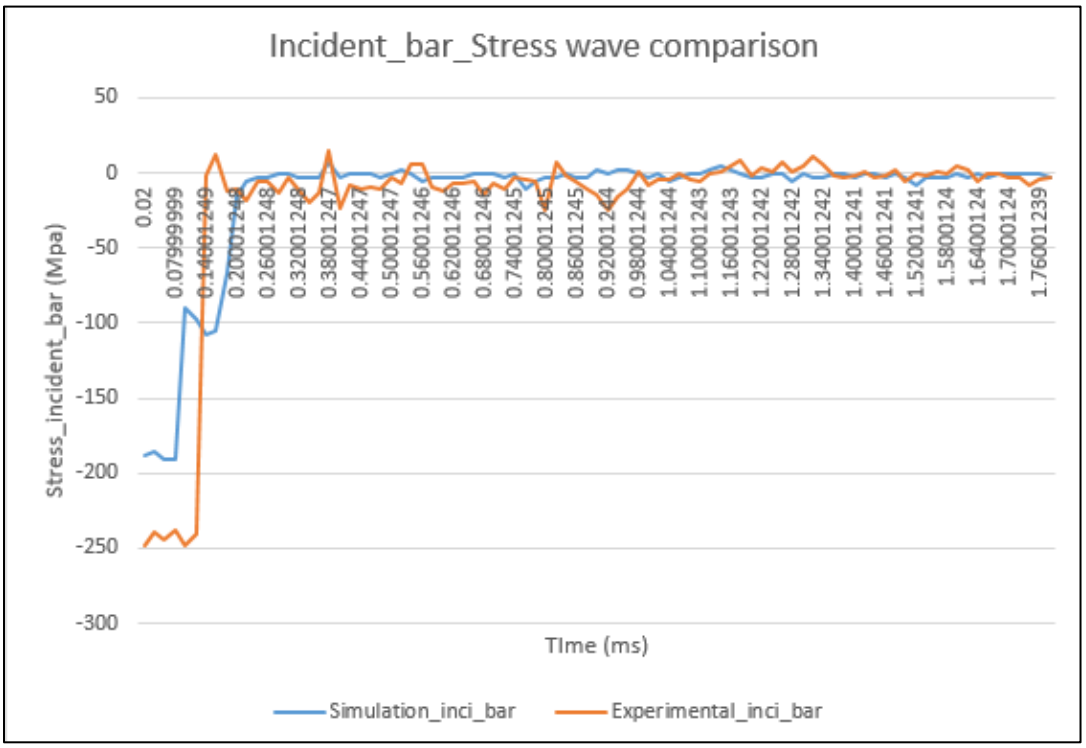

Figure 4-7: Superimposing Incidence pulse: Simulation and Experimental pulse

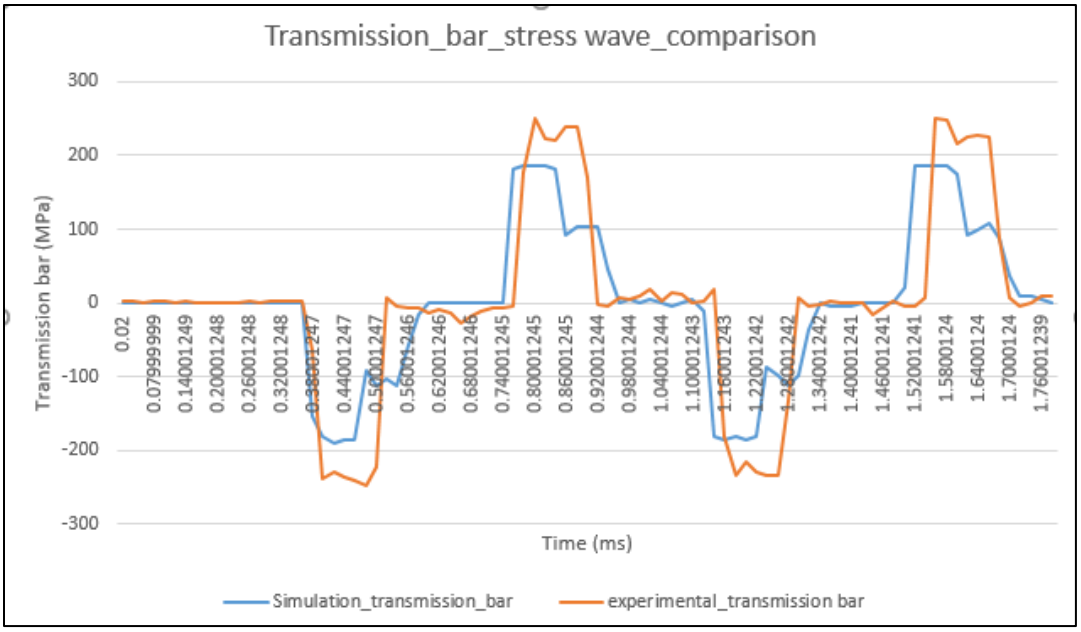

Figure 4-8: Superimposing Transmission pulse: Simulation and Experimental pulse

4.9 Comparison study of Simulation and Experimental Pulse

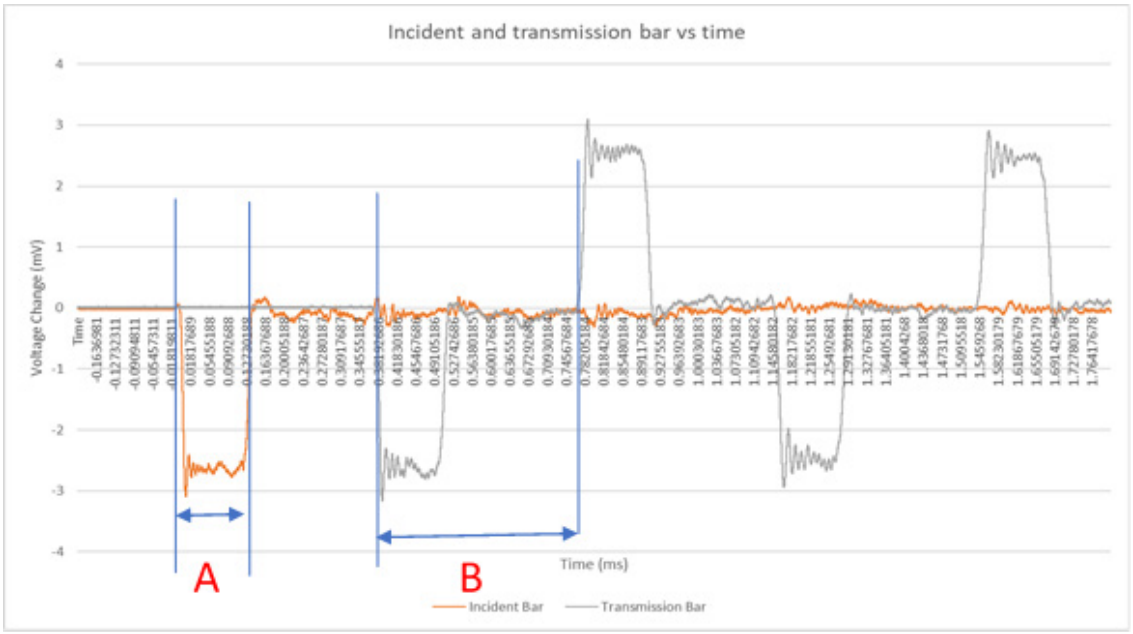

Figure 4-9: Analysis of test result waveform

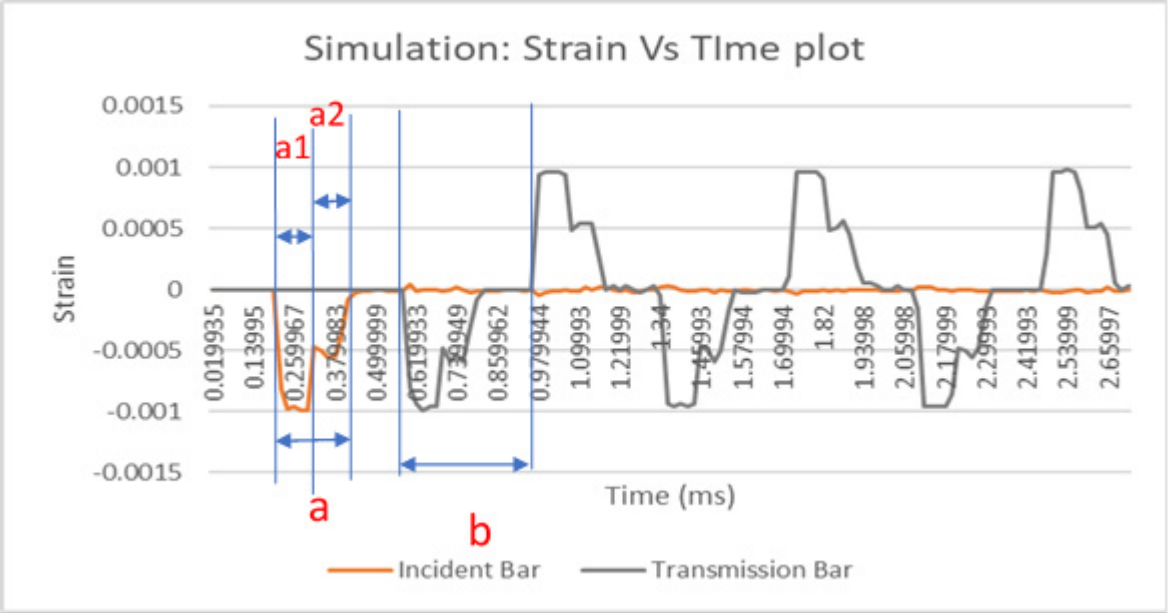

Figure 4-10: Analysis of Simulation waveform

Analyzing both the curve, following value is obtained:-

Experimental Result:-

A= Time between one wave passing: 0.13 ms

B= Distance between wave: 0.395 ms

Time step: $1.25*10^{-5}$ms

Simulation Result:

a= Time between one wave passing: 0.18ms

b= Distance between wave: 0.38ms

a1 = 0.1 ms

a2 = 0.08 ms

Time step (data recording): $2*10^{-2}$ms

Comparison shows that the value corresponding closely to the time axis. And also since the simulation and test data is only required for two pulse i.e. 0.8 ms. Result won't be influenced by time domain. But the significant difference exist in the stress value. For the simulation result, value appears in steps. [13] Some researcher proposes to use pulse shaper and have also studied the influence of different shape of pulse shaper. This has helped to achieve good correlation between testing and simulation as well as reduce oscillations.

4.10 Mesh Validation for SHPB set-up

Mesh validation study were carried out to account for the discrepancy in stress axis. All the analysis above were carried out with the element size of 2.286mm. Element size was reduced to see the impact in the simulation result. But this lead to more expensive analysis. The study was carried out for two purpose 1. To study the mesh impact in stress axis, 2. To optimize analysis to choose the right mesh for accuracy and analysis time. Mesh convergence study were further carried out for element size of 1.9, 1.5mm. Element size is same for radial and longitudinal axis.

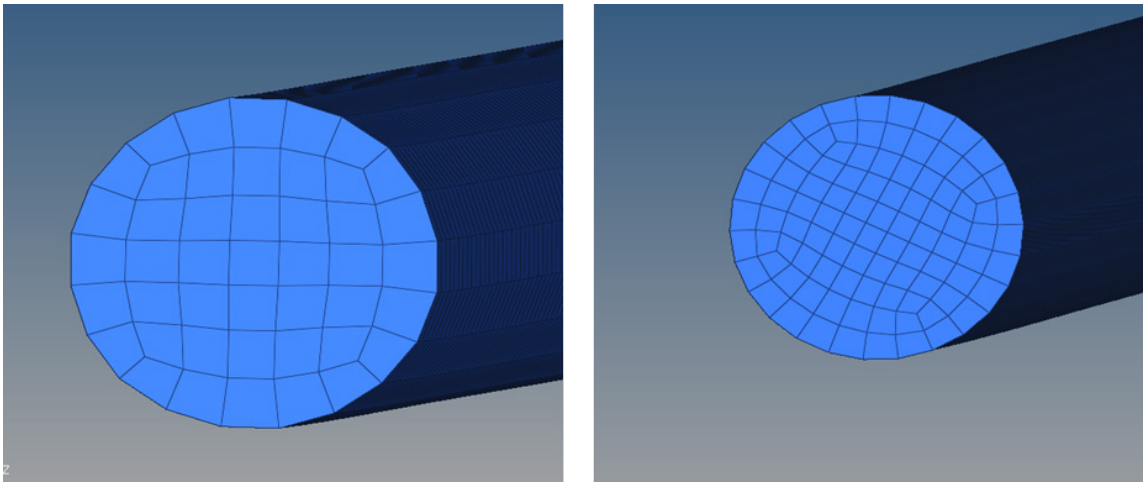

Figure 4-11: Mesh size for Mesh validation

Table 4-6: Mesh Validation storage size

Element Size (mm)	Run Time (hr)	Simulation File size (MB)	Total Result File Size (GB)
2.286	2	26	4
1.9	5	36	5.78
1.5	23	58	20

As can be easily seen from the table above, decreasing mesh size has significant impact on simulation run time. Image 4.13 shows the different mesh size selected. Result are evaluated from the strain gage method and superimposed on the test result to study the change observed in the numerical simulation. Image 4.14 shows the superimposed graph. As is clearly visible form the curve, there doesn't exist a significant change in the stress axis.

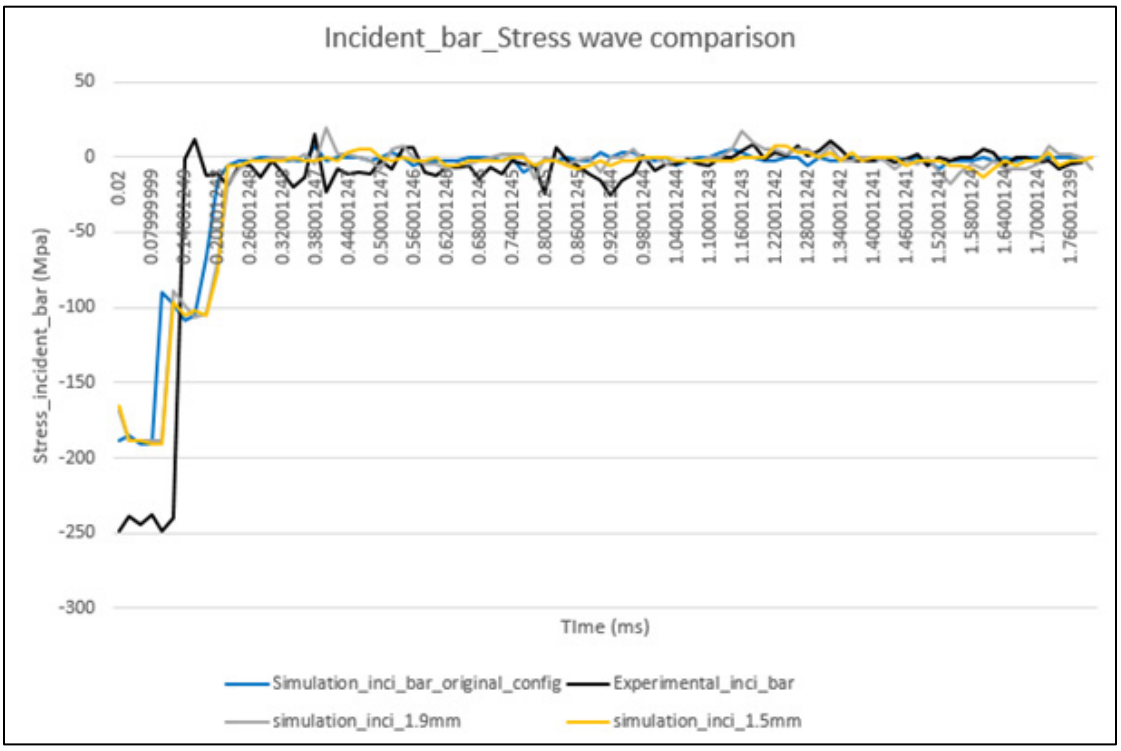

Figure 4-12: Mesh Validation Study: Superimposing Incidence pulse

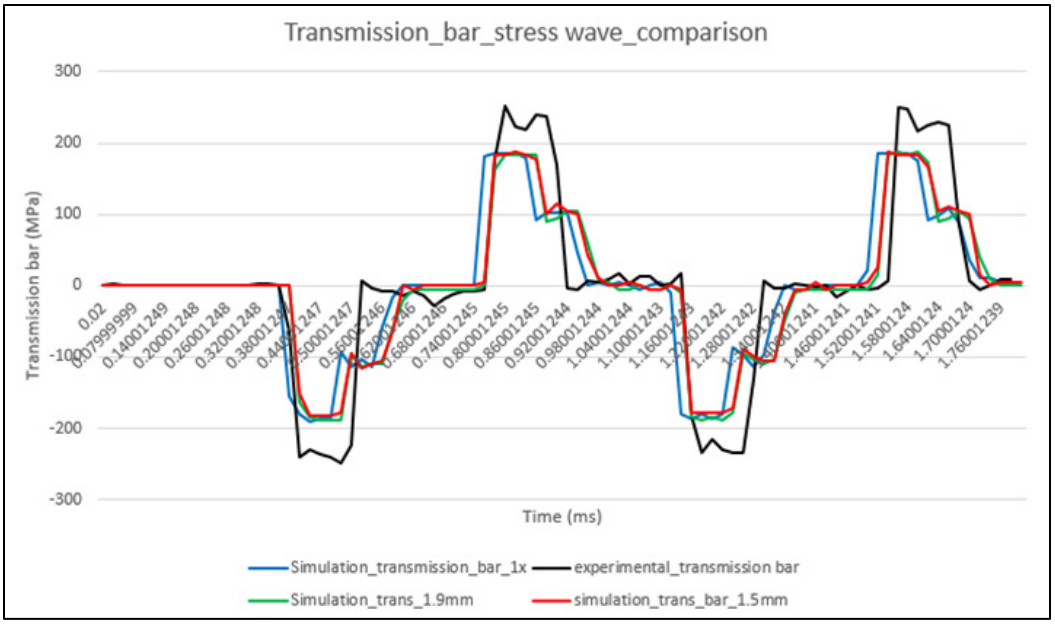

Figure 4-13: Mesh Validation Study: Superimposing Transmission pulse

4.11 Impact on incident pulse with or without sample

After having good confidence on the mesh size and idea on what to expect in the result. Incident pulse behavior were analyzed to observe if result vary changing the geometry setup. In other words, is there any change in incident pulse in set-up with or without samples? Two simulation were carried out a one with the sample and other taking off the sample. The input condition i.e. the velocity is kept constant in simulation. The result were again superimposed to study the behavior. Image shown below the superimposed curve. As can be easily seen, both the curve overlaps each other. And hence, geometry set-up difference with and without sample doesn't have an impact in incident pulse.

The simulation was further carried out for analysis of sample.

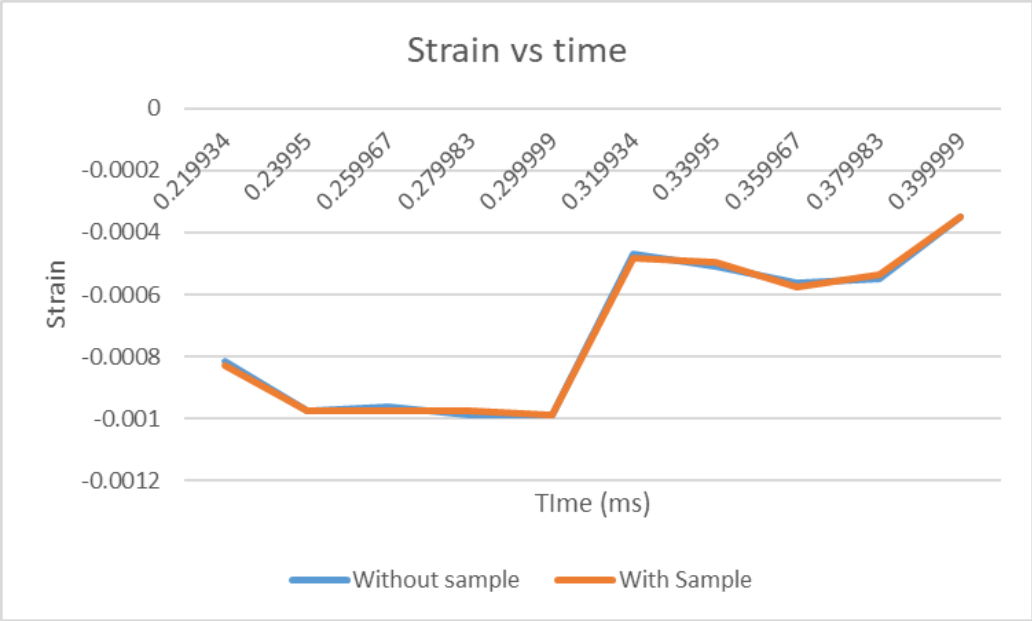

Figure 4-14: Incidence pulse with and without sample

4.12 Analysis of Sample

Sample size as used in the testing on borosilicate glass highlighted in chapter 3 has been used for numerical analysis. The sample Diameter is 0.317 in and length is 0.238 in. For the analysis of the sample, different approach is selected. LS-dyna software directly gives the stress in the sample with respect to time. The stresses obtained in the numerical analysis is compared experimental result.

Deriving constant may be complicated since lot of constant value has to be calculated. Numerous test have to be conducted to obtain test results. Several result are based on inferred to obtain material constant.

[2] Paper obtains a different approach for cost saving, fast paced and ease to development. Thorough literature review is carried out to find the available ceramic material definition. Several ceramics commonly used in ballistic material has been characterized. Literature highlight the constant derived for LS-dyna software for using in simulation. The characterized materials are Alumina (Al_2O_3), Boron Carbide (B_4C), Silicon Carbide (SiC), Aluminum Nitride (AIN) and silica float glass.

The idea behind this approach to find a ceramic corresponds closely to Borosilicate glass and that closely capture the feature of glass material.

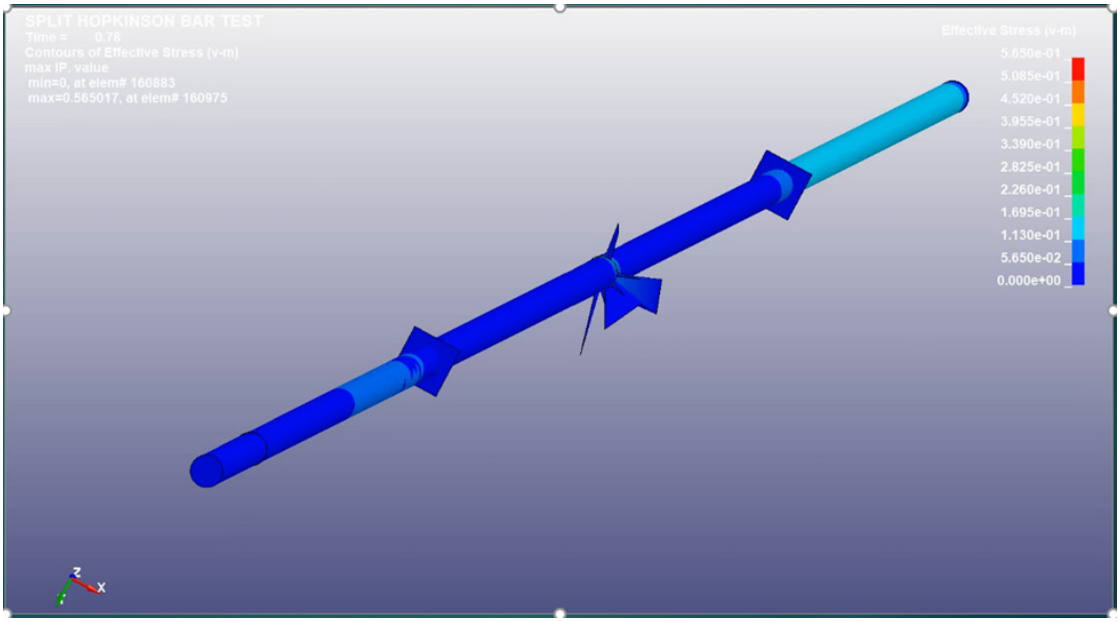

Figure 4-15: Simulation snapshot with glass sample

Table 4-7: Observation table for different ceramics

		15psi	25psi	35psi	40psi	50psi
Experimental Result	Max. Stress	541.89	692.00	951.53	926.22	1056.32
	Av. Stress	427.60	614.34	713.73	771.97	902.12
Silica Float	Max. Stress	681.71	267.77	635.16	852.47	343.48
	Av. Stress	216.58	98.25	171.53	230.39	97.29
B4C	Max. Stress	759.23	855.12	1098.03	1397.28	482.72
	Av. Stress	263.10	382.74	330.42	382.36	198.44
SiC	Max. Stress	759.14	1093.39	1201.79	1383.81	1785.77
	Av. Stress	504.75	1011.69	1149.97	1271.57	1525.14
AlN	Max. Stress	833.54	1017.27	1028.70	1185.67	482.72
	Av. Stress	752.55	950.97	528.63	398.06	198.44
Al2O3	Max. Stress	48.74	444.43	310.60	88.10	52.86
	Av. Stress	31.49	132.77	101.07	45.56	41.62

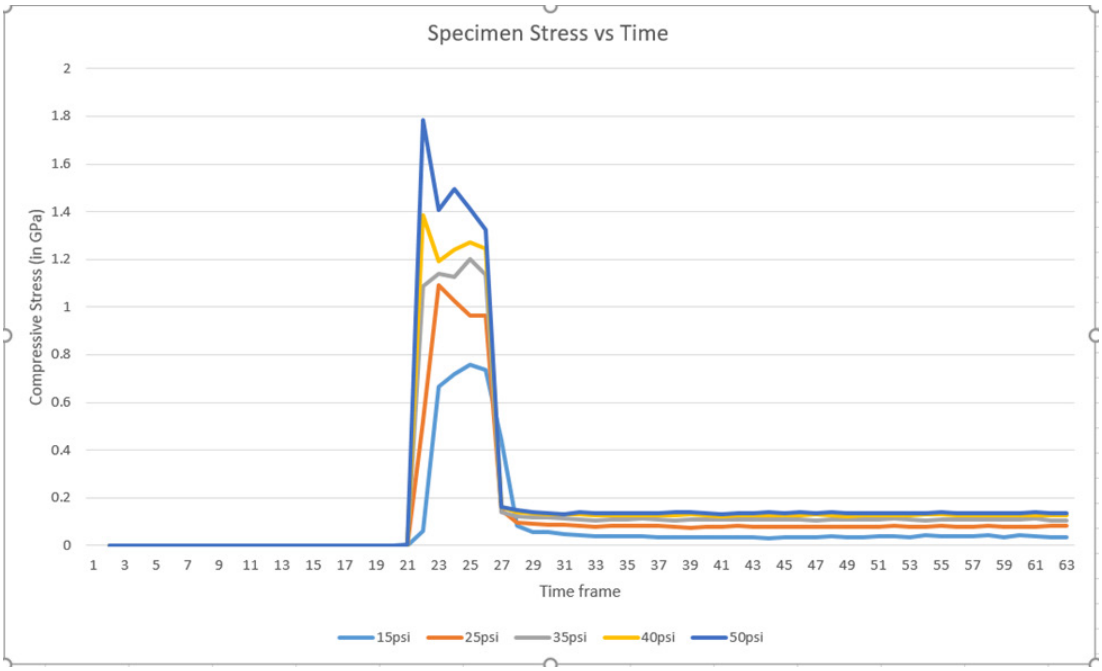

Figure 4-16: Silicon Carbide Specimen result

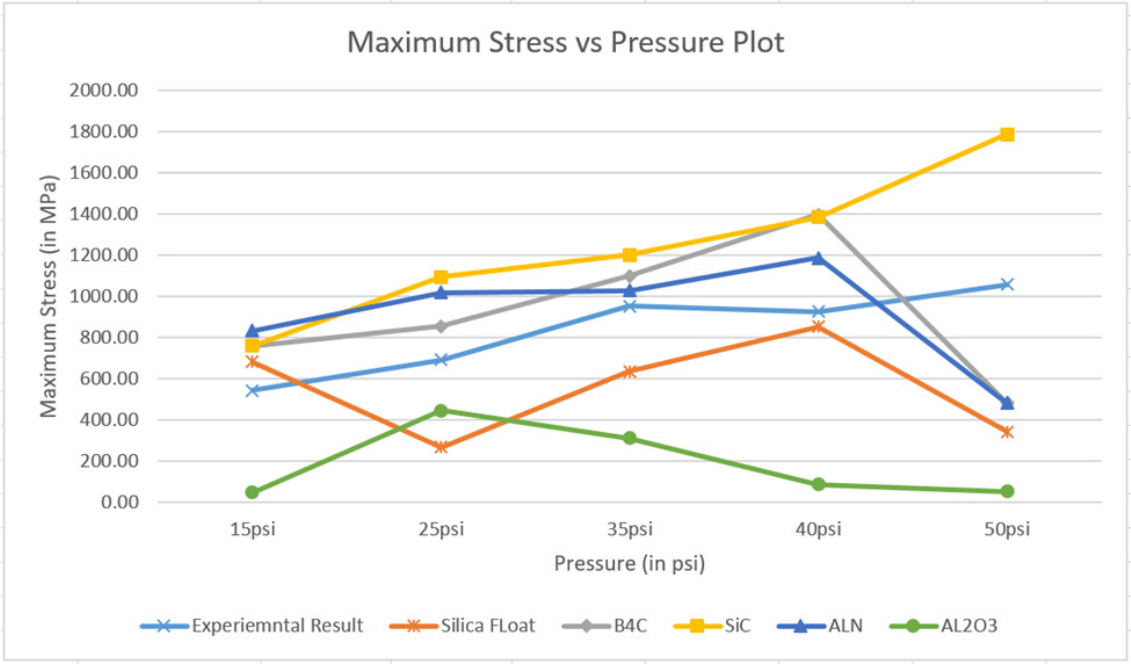

Figure 4-17: Sample analysis maximum stress vs pressure plot

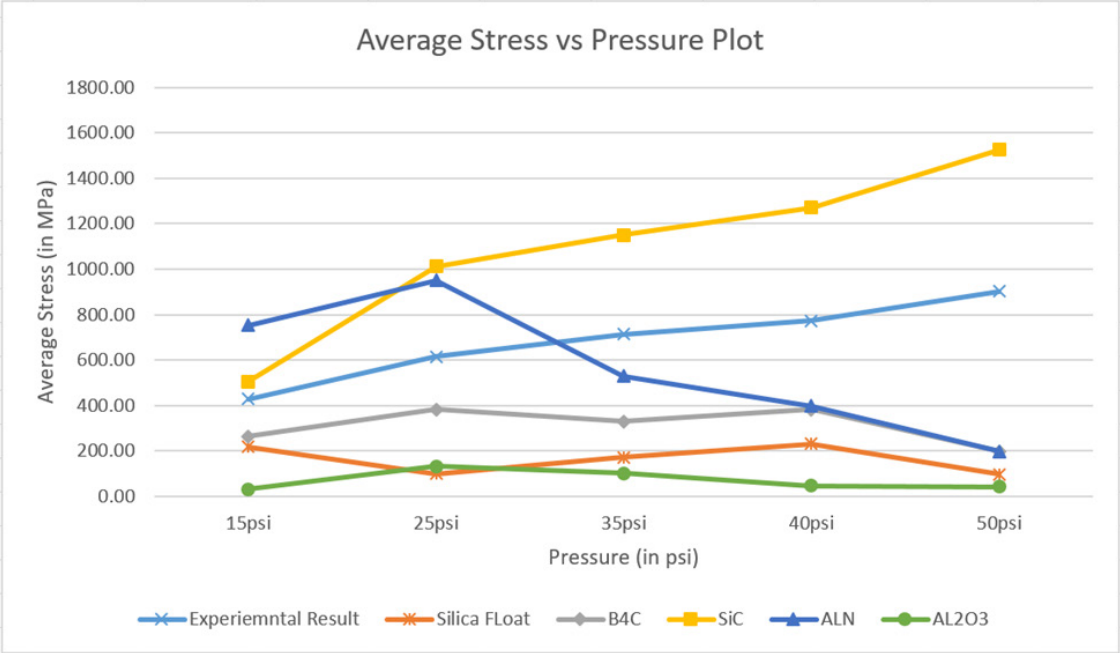

Figure 4-18: Sample analysis average stress vs pressure plot

Experimental test result shows the failure in the time frame of 0.0008-0.001 ms. The simulation result for average stress above which corresponds to averaging 4-5 time step. Whereas maximum stress is corresponding to maximum value reached during simulation or testing.

Observation from the result are as follows 1. Average stress may be a good measure for correlating since less variation is observed in the data. 2. Test result shows a upward trend with increase in impact velocity. Only SiC occur to follow the same trend. But has a very high strength difference in magnitude. 3. Silica float glass and Al2O3, shows very low strength under impact loading. 4. The test result is closest to B4C and ALN.

The result could be improved by following method 1. Having to compare result over a wide range of strain rate. 2. Experimental result shows a change in the slope for float in flow stress at around strain rate of 100-200/s. Since the test is carried out in that range, it may be prone to errors. 3. Specimen analysis could be improved by studying specimen reaction with different material and selecting appropriate mesh.

5 Conclusion

Material model is a crucial element for effectively characterizing FEA simulation subsequently resulting in close agreement with naturally occurring phenomena. Understanding the dynamics of ceramic materials under ballistic impact and validation of experimental measurements with simulation results are essential to obtain a fairly accurate material model. The findings of this paper will be summarized under following heads.
Dynamic of Ceramic under ballistic impact: It is guided by the interplay in the difference of strength between magnitude of comprehensive wave and dynamic strength of material. If the former is greater cracks propagates whereas otherwise material fails in reflected tensile wave. LS-Dyna MAT_110 is selected for simulation which incorporates strain rate effects, failure criteria, damage effects and tension handled differently than compression.

Dynamic Strain rate testing: Split Hopkinson Pressure Bar (SHPB) test on 1018 cold rolled steel obtained good correlation with the literature result available. SHPB test on borosilicate glass showed steep increase in the Stress developed in the sample with increase in velocity of striker. Use of shim during testing, interfered with the test result.

Numerical Simulation model: SHPB setup is modeled in hyper mesh and simulated in LS-dyna. Loading pulse is analyzed to validate the model. Good correlation in the wave form is observed, but the stress developed in numerical simulation was approximately 20% less than the actual test. Specimen was analyzed for five ceramic model based on the available literature model. Fracture was observed in the simulation result as well for higher input pressure. Same trend was observed for silicon carbide, but other material didn't followed the same trend.

Cross validation of testing and simulation can be a good method to have good correlational model.

6 Future Work Recommendations

Result shows a gap in the correlation between the simulation and actual result. The reason may have been because of various process simplification adopted in the development. Carefully studying their impact and incorporating it appropriately can provide the required correlation. These are the few key point that can be considered for improving the correlation between model:-

Experimental:-

1. Specimen dimension for various L/D ratio could be considered for steadier increase in strain rate change with change in input pressure.

2. Spall testing or plate impact could be incorporated for higher order strain rate.

3. Study of impact of shim and using appropriate shim could be key for improving variation between samples.

4. Image correlation could be an effective measure the study the growth of crack.

5. Sample preparation to ensure parallelism and pre analysis of sample for defect could provide a basis for predicting test result.

Simulation:-

1. Model validation with known result could be incorporated for having good confidence in model.

2. Model behavior with higher strain rate could be key, since MAT 110 was developed for ballistic impact. Having to compare result over a wide range of strain rate could also provide good measure.

3. Experimental result for float glass shows a high rate of flow stress change with strain rate. The model variation for different strain rate could provide good measure for model validation.

4. Specimen analysis could be improved by studying specimen reaction with different material and selecting appropriate mesh.

5. Approach to incorporate lower time step could help in better validation with experimental result.

7 Reference List

1. Zhang, X., H. Hao, and G. Ma, *Dynamic material model of annealed soda-lime glass.* International Journal of Impact Engineering, 2015. **77**: p. 108-119.

2. Cronin, D.S., et al. *Implementation and validation of the Johnson-Holmquist ceramic material model in LS-Dyna*. in *Proc. 4th Eur. LS-DYNA Users Conf*. 2003.

3. Gandhi, S.S., *Simulation of Crack Pattern on Borosilicate Glass Cylinder on Pellet Impact.* 2017.

4. Holmquist, T.J., G.R. Johnson, and C.A. Gerlach, *An improved computational constitutive model for glass.* Philosophical Transactions of the Royal Society A: Mathematical, Physical and Engineering Sciences, 2017. **375**(2085): p. 20160182.

5. Chocron, S., et al., *Characterization of confined intact and damaged borosilicate glass.* Journal of the American Ceramic Society, 2010. **93**(10): p. 3390-3398.

6. Alexander, C.S., et al., *Changes to the shock response of fused quartz due to glass modification.* International Journal of Impact Engineering, 2008. **35**(12): p. 1376-1385.

7. Holmquist, T.J. and A.A. Wereszczak, *The internal tensile strength of a borosilicate glass determined from laser shock experiments and computational analysis.* International Journal of Applied Glass Science, 2014. **5**(4): p. 345-352.

8. Chocron, S., et al., *Damage threshold of borosilicate glass under plate impact.* Journal of Dynamic Behavior of Materials, 2016. **2**(2): p. 167-180.

9. McIntosh, G., *The Johnson-Holmquist ceramic model as used in LS-DYNA2D*. 1998, DEFENCE RESEARCH ESTABLISHMENT VALCARTIER (QUEBEC).

10. *LS-DYNA R10.0 (r:9024).* 2017.

11. *REL. SURE-PULSE™ Software version 1.9.x.*

12. Naghdabadi, R., M. Ashrafi, and J. Arghavani, *Experimental and numerical investigation of pulse-shaped split Hopkinson pressure bar test.* Materials Science and Engineering: A, 2012. **539**: p. 285-293.

13. Panowicz, R., J. Janiszewski, and K. Kochanowski, *Influence of pulse shaper geometry on wave pulses in SHPB experiments.* Journal of Theoretical and Applied Mechanics, 2018. **56**(4): p. 1217-1221.